The effect of intraspecific variation and heritability on community pattern and robustness

György Barabás & Rafael D'Andrea

Ecology Letters, in press

Abstract

Intraspecific trait variation is widespread in nature, yet its effects on community dynamics are not well understood. Here we explore the consequences of intraspecific trait variation for coexistence in two- and multispecies competitive communities. For two species, the likelihood of coexistence is in general reduced by intraspecific variation, except when the species have almost equal trait means but different trait variances, such that one is a generalist and the other a specialist consumer. In multispecies communities, the only strong effect of nonheritable intraspecific variation is to reduce expected species richness. However, when intraspecific variation is heritable, allowing for the possibility of trait evolution, communities are much more resilient against environmental disturbance and exhibit far more predictable trait patterns. Our results are robust to varying model parameters and relaxing model assumptions.

Statement of authorship: GB and RD conceived of the study and developed the model framework; RD designed tests of trait patterns; GB designed tests of community robustness; GB and RD wrote the manuscript.

1 Introduction

Despite the persistent (and generally valid) complaint that not enough attention is given to within-species diversity, it is now in fact well established in mainstream ecology that intraspecific trait variation (ITV) can have important ecological consequences (Hughes et al. 2008, Clark 2010, Bolnick et al. 2011, Violle et al. 2012). What is not yet clear is how much ecological insight we actually gain (or lose) by ignoring this variation, looking only at trait means. Do we get the "basic picture", which is then refined and made more precise by accounting for intraspecific trait variation (Siefert 2012)? Or do we miss certain aspects of the community entirely? In the literature, the importance of intraspecific variation is often equated with its prevalence. A recent study by Siefert et al. (2015) estimates that, on average, 25% of all trait variation in plant communities is intraspecific. The same study gives "general guidelines for when intraspecific trait variation is likely to be substantial *and therefore important to consider* in plant community and ecosystem studies" (our emphasis). Similarly, Albert et al. (2011) provide a practical guide for when intraspecific trait variation should be included in trait-based studies; their criteria are also based on estimating intraspecific variation prevalence. Our goal here is to study the importance of intraspecific variation for community dynamics and in particular for coexistence, based not on prevalence but impact on species richness, community pattern, and robustness. Critically, once there is individual variation within a species, part of that variation may be heritable. We therefore also consider the possibility of nonzero heritability, leading to the evolution of species traits.

Consequences of intraspecific variation for the dynamics of single populations have been long studied (Metz and Diekmann 1986, Caswell 2001, de Roos and Persson 2013). At the community level, arguments

about the consequences of within-species trait diversity abound. The most common stance is that such variation blurs species boundaries, though authors disagree about whether this would promote coexistence by facilitating ecological equivalence (Hubbell 2005) or hinder it by erasing coexistence-enhancing species differences (Taper and Case 1985).

There are also some deeper theoretical explorations of the community consequences of intraspecific variation. Lichstein et al. (2007) looked at the consequences of individual variation in competitive ability, assuming that lower mean performance is accompanied by higher intraspecific variation (mean-variance tradeoff), and find that this enhances coexistence, albeit only slightly so. In addition, community models with explicit life histories have shown strong community consequences of intraspecific age, stage, or physiological structure (Moll and Brown 2008, van Leeuwen et al. 2014). Treating every species as a structured population and incorporating interactions between life stages is a very general and powerful way of modeling species with individual variation (see de Roos and Persson 2013, Vindenes and Langangen 2015 for general formalisms), but it can get arbitrarily complicated, depending on the idiosyncrasies of the individual life histories of each species modeled. As such, this approach may not be the most convenient to draw general conclusions from. Another, relatively simple but still explicitly trait-based approach is taken in classic and some more recent studies of character displacement (Roughgarden 1976, Slatkin 1979, 1980, Taper and Case 1985, Vasseur et al. 2011). Here trait variation is driven by quantitative genetics and simple interactions defined by those traits. While these studies draw important conclusions about how intraspecific variation shapes competitive communities, they have traditionally focused on the evolutionary and not the ecological aspect of the problem.

All the above approaches consider only two, or at most a handful of species. To our knowledge, only two previous studies have looked at the effects of intraspecific variation on coexistence in multispecies communities. Vellend (2006) simulated communities along a unidimensional trait axis, with clonal reproduction and Lotka–Volterra competitive interactions. He found that within-species trait diversity promotes community-wide coexistence. However, one problematic aspect of this study is that, since all individuals breed true, the distinction between intra- and interspecific variation is purely nominal. It therefore does not yield deep insights into the structure of communities where conspecific individuals can exchange genetic material. Yamauchi and Miki (2009) modified the model to address this problem, incorporating a finite-locus model of genetics following the Shpak-Kondrashov hypergeometric model of inheritance (Shpak and Kondrashov 1999), instead of simple clonal reproduction. They found, in contrast to Vellend (2006), that intraspecific variation only promotes species diversity under a very restricted set of circumstances.

In this work we aim to give a comprehensive view of the consequences of intraspecific trait variation on coexistence in both two- and multispecies communities. We consider both heritable and nonheritable intraspecific variation in the framework of quantitative genetics (Lande 1976, Slatkin 1979, Bulmer 1980, Falconer 1981), coupled with Lotka–Volterra-style ecological interactions (Roughgarden 1976, Slatkin 1980, Taper and Case 1985, Schreiber et al. 2011, Vasseur et al. 2011). In contrast to Vellend (2006) and Yamauchi and Miki (2009), we do not focus exclusively on species richness as a measure of whether coexistence is promoted. Rather, we additionally consider community pattern and community robustness against environmental perturbations. We find that the only strong and general consequence of intraspecific variability *per se* is that it reduces species richness, while its effect on trait patterns and community robustness is very small. In contrast, effects are huge when part of the intraspecific variance is heritable. This allows species to evolve their trait values towards local optima, thus alleviating historical constraints and leading to communities that are far more robust and have far more regular trait patterns than corresponding communities with zero heritability. We check and confirm that our results are not sensitive to our particular choice of model parameters and simplifying assumptions such as the infinite-locus model of quantitative genetics.

2 The model

We assume individuals of a species vary along a unidimensional trait of interest. The phenotypic distribution of this trait is considered in the quantitative genetic limit (Lande 1976, Bulmer 1980, Falconer 1981, Schreiber et al. 2011, Vasseur et al. 2011). In this limit, each of infinitely many loci contributes an infinitesimal additive value to the trait, on top of normally distributed environmental noise. Under these assumptions, the distribution $p_i(z,t)$ of species i's trait value z at any moment of time t is normal, with a total phenotypic variance σ_i^2 that does not change in response to selection (Supporting Information, Section 1.1):

$$p_i(z,t) = \sqrt{\frac{1}{2\pi\sigma_i^2}} \exp\left(-\frac{(z-\mu_i(t))^2}{2\sigma_i^2}\right) \tag{1}$$

where $\mu_i(t)$ is the mean trait value at time t. The total phenotypic variance is the sum of the additive genetic variance and an independent environmental variance, which we assume is species-specific but does not change in time. The heritability h_i^2 in species i is defined as the ratio of the additive and the total phenotypic variance (Falconer 1981). If species i has total population density $N_i(t)$ at time t, then $N_i(t)p_i(z,t)\mathrm{d}z$ is the population density of individuals with phenotype values between z and $z+\mathrm{d}z$.

Since the shape and variance of the trait distribution does not change in the quantitative genetic limit, the full distribution $N_i(t)p_i(z,t)$ can be recovered from just tracking the population density and mean trait value of each species in time. These equations read

$$\frac{\mathrm{d}N_i(t)}{\mathrm{d}t} = N_i(t) \int r_i(\vec{N},\vec{p},z,t)p_i(z,t)\,\mathrm{d}z \tag{2}$$

$$\frac{\mathrm{d}\mu_i(t)}{\mathrm{d}t} = h_i^2 \int (z-\mu_i(t))r_i(\vec{N},\vec{p},z,t)p_i(z,t)\,\mathrm{d}z \tag{3}$$

(Supporting Information, Section 1.2), where $r_i(\vec{N},\vec{p},z,t)$ is the per capita growth rate of species i's phenotype z, defined by the ecological interactions of the community (it is density- and frequency-dependent, therefore written as a function of the vector of abundances $\vec{N}$ and trait distributions $\vec{p}$). The above equations therefore provide the general framework for the eco-evolutionary dynamics in the presence of intraspecific trait variation that will hold regardless of the ecological details.

Ecological interactions are assumed to depend only on phenotype, not on species identity. We use the Lotka–Volterra model in the quantitative genetic limit (Roughgarden 1976, Slatkin 1979, 1980, Taper and Case 1985, Vasseur et al. 2011), where the fitness of any individual with phenotype z depends both on its absolute position and its distance from any other individual along the trait axis, summed over all individuals:

$$r(\vec{N},\vec{p},z,t) = b(z) - \sum_{j=1}^{S} N_j(t) \int a(z,z')p_j(z',t)\,\mathrm{d}z' \tag{4}$$

(Supporting Information, Section 2.1). Here $b(z)$ is the maximum population growth an individual with phenotype z would achieve were it to reproduce clonally, S is the number of species, and $a(z,z')$ is the interaction kernel—the effect of an individual with phenotype z' on the growth rate of another individual with phenotype z. Substituting Eq. (4) into the general equations (2) and (3), we get

$$\frac{\mathrm{d}N_i(t)}{\mathrm{d}t} = N_i(t)\left(b_i(t) - \sum_{j=1}^{S} \alpha_{ij}(t)N_j(t)\right) \tag{5}$$

$$\frac{\mathrm{d}\mu_i(t)}{\mathrm{d}t} = h_i^2\left(\overline{b}_i(t) - \sum_{j=1}^{S} \beta_{ij}(t)N_j(t)\right) \tag{6}$$

Here $b_i(t)$ is a species-level intrinsic growth rate, $\alpha_{ij}(t)$ are species-level competition coefficients, $\overline{b}_i(t)$ quantifies the evolutionary pressure on species i caused by growth, and $\beta_{ij}(t)$ quantifies the evolutionary pressure on species i caused by competition with species j. Given the functions $a(z,z')$ and $b(z)$, these four ingredient functions can be obtained analytically by evaluating appropriate integrals (Supporting Information, Section 2). In our study, the interaction kernel $a(z,z')$ is Gaussian with competition width ω:

$$a(z,z') = \exp\left(-\frac{(z-z')^2}{\omega^2}\right) \tag{7}$$

We assume $b(z)$ is positive on an interval $[-\theta, \theta]$ but zero outside; $\theta > 0$ is therefore the effective half-width of the trait axis. Biologically, this means that any trait value falling outside this region is too extreme to efficiently forage for any of the available resources and thus achieve positive growth. Within the range $[-\theta, \theta]$ however, we consider three alternative forms: $b(z) = 1$ (rectangular), $b(z) = 1 - z^2/\theta^2$ (quadratic), and $b(z) = (z+\theta)/(2\theta)$ (asymmetric triangular).

3 Two-species case

A model predicts coexistence if it has an equilibrium where all species abundances are positive (feasibility; Barabás et al. 2012, Rohr et al. 2014), the equilibrium is dynamically stable (stability), and the equilibrium remains stable and feasible under a sufficiently wide range of environmental conditions (robustness; Barabás et al. 2014). The two-species case of the quantitative genetic Lotka–Volterra model is particularly interesting as it gives insight into the coexistence-affecting role played by intraspecific variation. In the two-species version of the model with zero heritability, any feasible equilibrium is always globally stable (Supporting Information, Section 3.1). Therefore, analyses of feasibility and robustness are sufficient to determine whether species coexist.

Feasibility in our model is characterized by pairs of intrinsic growth rates (b_1, b_2) that lead to positive equilibrium densities. Robustness may then be characterized by the fraction of growth rate combinations

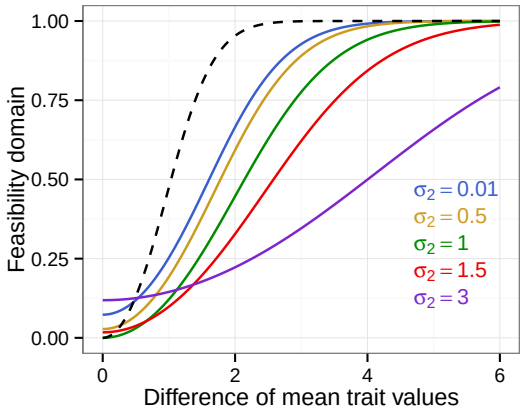

Figure 1: The fraction of intrinsic growth rate combinations out of all possible ones that lead to coexistence (the feasibility domain), as a function of mean trait distance and intraspecific variability. The competition width is $\omega = 1.1$ for all cases. The dashed black line is the reference case with no intraspecific variation: $\sigma_1 = \sigma_2 = 0$. For all solid curves, $\sigma_1 = 1$; colors denote different values of σ_2 (see legend). Except for very small differences in mean trait, the case with no intraspecific variation leads to the largest feasibility domains. For very small mean trait difference, the feasibility domain is larger for bigger differences in σ_1 and σ_2. Intraspecific variation therefore promotes the coexistence of tightly packed species, but only if their σs are sufficiently different.

leading to feasibility, out of all possible combinations. This is the feasibility domain Ξ. We derive a formula for Ξ in the Supporting Information (Eq. 3.10):

$$\Xi = \frac{2}{\pi}\left[\arctan\left(e^{\frac{d^2}{2\sigma_1^2+2\sigma_2^2+\omega^2}}\sqrt{\frac{2\sigma_1^2+2\sigma_2^2+\omega^2}{4\sigma_2^2+\omega^2}}\right) - \arctan\left(e^{-\frac{d^2}{2\sigma_1^2+2\sigma_2^2+\omega^2}}\sqrt{\frac{4\sigma_1^2+\omega^2}{2\sigma_1^2+2\sigma_2^2+\omega^2}}\right)\right]. \quad (8)$$

Note that there are alternative ways of characterizing robustness (Supporting Information, Section 3.2); they yield qualitatively identical results.

The predictions of the formula are shown on Figure 1 as a function of the distance between species' mean traits, for various values of the intraspecific variances (Supporting Information, Section 3.2). There are two main messages. First, unless species' trait means are very close, more intraspecific variation always leads to a smaller feasibility domain, diminishing the chances of coexistence. Second, for very similar mean traits, having sufficiently different trait variances promotes coexistence, and this effect is larger for more substantial differences between σ_1 and σ_2. This can be understood in terms of Figure 2: the overlap between two species having similar trait means is reduced by a difference in variances (phenotypic subsidy; Bolnick et al. 2011). Since Eq. (8) is valid for all trait means and variances, it handles these two modes of coexistence in a unified way. Moreover, the formula allows for the direct comparison of coexistence with- and without intraspecific variability (Figure 1, solid versus dashed lines).

There is also an evolutionary aspect to this problem. So far we have treated the mean traits of the species as parameters. If heritabilities are nonzero however, these will be subject to change, governed by Eq. (6). If the intraspecific variances are sufficiently different, the two species can converge and end up having equal mean trait values (Roughgarden 1976, Slatkin 1979, 1980, Taper and Case 1985; Supporting Information, Section 3.3). Although strictly speaking the evolution of equal trait means is only possible via symmetric intrinsic growth functions $b(z)$, this result is robust to introducing an asymmetry in $b(z)$ in the sense that the difference in mean trait values at the eco-evolutionary equilibrium will be much smaller than either of the intraspecific standard deviations (Supporting Information, Section 3.4). In the parlance of Taper and Case (1985), character displacement will not be substantial.

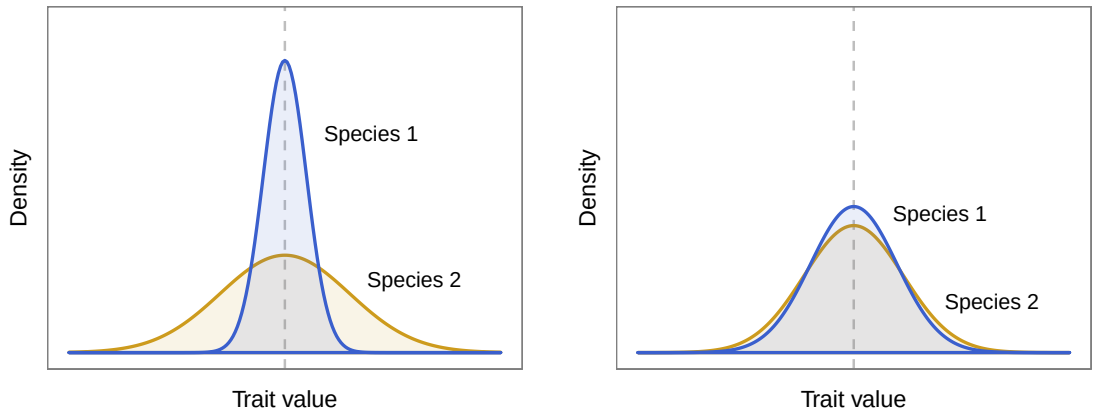

Figure 2: Left: The intensity of interspecific competition between two species with the same mean trait is lowered if their trait variances are different. The reason is that the species with the higher variance has individuals that do not overlap with individuals of the the other species. This way those individuals avoid competition by accessing different resources. Right: when two species with the same mean trait have very similar intraspecific variances, the overlap in individuals is not reduced substantially, leading to nonrobust coexistence. The dashed gray line indicates the species' mean trait position.

In summary, a rule of thumb for the effect of intraspecific variation on two-species coexistence is that it is *harmful*, considerably narrowing the range of parameter combinations allowing for coexistence compared with the no-variation scenario. The only exception is when the trait means are very similar and the standard deviations are sufficiently different. Due to this possibility, much tighter species packing may in principle be achieved, provided that one species is a generalist and the other a specialist consumer. Species can either be segregated in their trait means or in their trait variances. Focusing exclusively on the mean trait may lead to the false conclusion that two species are coexisting without niche segregation.

4 Multispecies case

4.1 Motivating examples

Figure 3 shows nine communities at equilibrium: without intraspecific variation (left column), with nonheritable variation (center column), and heritable variation (right column; $h^2 = 0.1$ for all species). The σ_i in the center and right columns are identical in each row and are uniformly drawn from $[0.1, 0.3]$ (top row), $[0.01, 0.05]$ (middle row), and $[0.01, 0.3]$ (bottom row). Rows differ in the form of $b(z)$ (top: rectangular; middle: quadratic; bottom: triangular). Otherwise, all panels have the same parameters and initial conditions. In each row, the number of persisting species is highest in the absence and intermediate in the presence of nonheritable intraspecific variation, and lowest in the presence of heritable variation. In addition to reduced species richness, positive heritability leads to much more regular spacing between surviving species, with no two species very closely packed along the trait axis.

These observations outline the questions pertinent to the effects of intraspecific variation and heritability on multispecies coexistence. How does intraspecific variation affect species richness, and is the effect different for zero and nonzero heritability? Are species more evenly spaced in the case of nonzero heritability? Do we ever observe trait convergence in multispecies communities? How does intraspecific variation affect our ability to detect the signature of competition in field-collected trait data? And what is the effect of intraspecific variation and heritability on the community's ability to withstand environmental perturbations?

4.2 The simulation scheme

To address these questions, we use data generated by the quantitative genetic Lotka–Volterra model described in Section 2. Our simulations are organized into sets. Within each set there are 90 simulations, each with a different choice of parameters but the same initial conditions. All simulations start with $S = 51$ species, $\theta = 1/2$, and initial abundances equal to one. The initial trait means $\mu_i(0)$ are uniformly sampled from the interval $[-\theta, \theta]$. Then, the set is generated by varying the following parameters independently:

- Heritability: all species share the same $h_i^2 \equiv h^2$, equal to either 0, 0.1, or 0.5.
- Shape of $b(z)$: either rectangular, quadratic, or triangular (Section 2).
- Competition width ω: either 0.1, 0.15, or 0.2.
- Degree of intraspecific variability: species' intraspecific standard deviations σ_i are uniformly sampled from either $[0, 0]$ (no variation), $[0.01, 0.05]$ (low levels of variation), $[0.01, 0.3]$ (mixed levels of variation), or $[0.1, 0.3]$ (high levels of variation).

Combinations with zero intraspecific variability ($\sigma_i = 0$) but nonzero heritability are discarded, since species cannot evolve without intraspecific variation. This results in (three heritabilities) $\times$ (three intrinsic growth functions) $\times$ (three competition widths) $\times$ (four intraspecific variability levels) $=$ 108 different simulations within a set, minus the 18 cases with nonzero heritabilities but zero intraspecific variation, for a total of 90

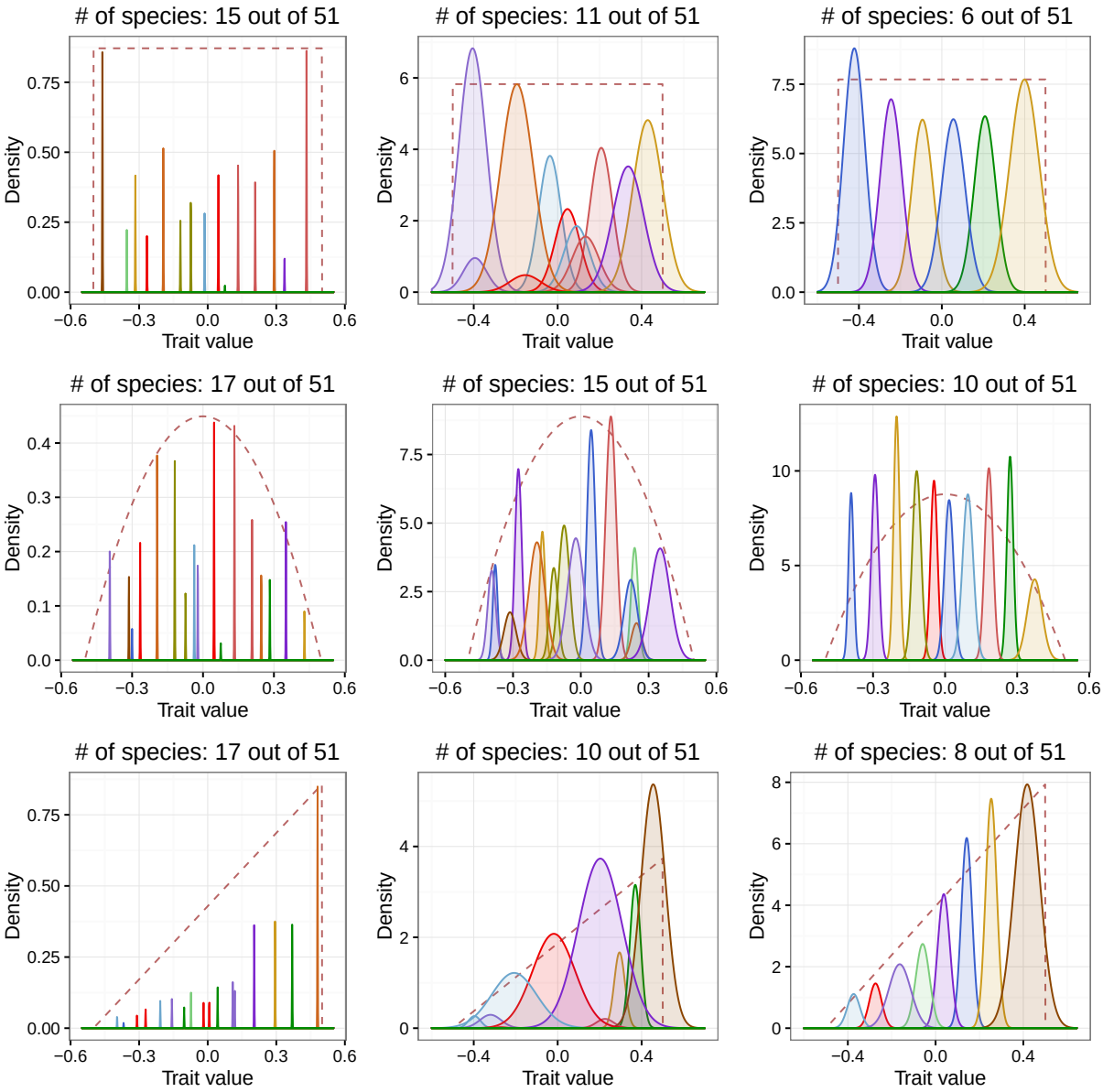

Figure 3: Equilibrium state of simulated communities. Columns correspond to no intraspecific variability (left), nonheritable variability (middle), and heritable variation (right). Rows correspond to different shapes of $b(z)$ (red dashed lines; not to scale): rectangular (top), quadratic (middle), and triangular (bottom). In all panels, $\theta = 0.5$, $\omega = 0.1$, initial mean trait positions are uniformly sampled from $[-\theta, \theta]$, and the initial species richness is $S = 51$. Parameters and initial conditions are identical between middle and right columns, except for heritability. The left column is exactly as the middle column except all σs are zero. Plot headers show the number of surviving species. Ordinates show actual population density in left column; in the center and right columns, the area under the species trait distributions yields the densities. When heritability is nonzero (right), species space themselves out more evenly than when they cannot change their initial mean trait positions.

different combinations. A total of 100 such sets are generated altogether, each determined by the set of initial trait means.

Note that both the initial trait positions $\mu_i(0)$ and the intraspecific standard deviations for each of the three nonzero cases (low, mixed, and high levels) are pre-generated for each set prior to simulations and so are kept the same within each set. This way we can disentangle the effects of initial conditions from those of the parameters. Each simulation ran for 10^{10} time units, more than enough in every case to reach eco-evolutionary equilibrium. Species with final density lower than an extinction threshold of $N_{\text{ext}} = 10^{-3}$ were removed from the community.

4.3 Species richness

Figure 4 shows species richness results across all our sets. Compared to the $\sigma_i = 0$ case (top left subplot), introducing intraspecific variation with zero heritability lowers the expected diversity (top row). With positive heritability, the equilibrium number of species further decreases, and becomes more predictable. Comparing the panels of Figure 3 reveals that species become more evenly spaced if they are allowed to evolve, which also results in more predictable species counts (see also Section 4.4).

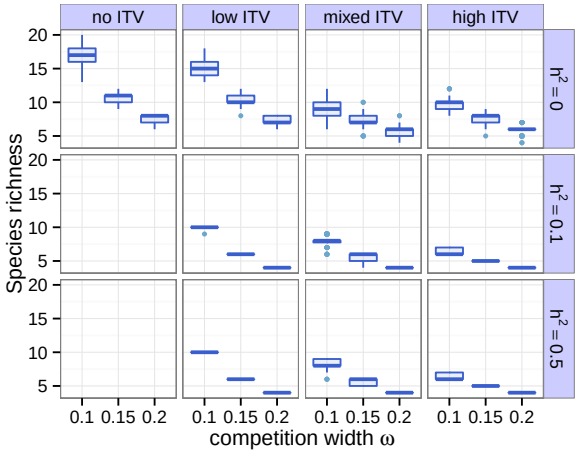

Figure 4: The effect of intraspecific variation and heritability on species richness. Rows of subplots show different heritability values; columns show different levels of intraspecific trait variability (ITV). The ordinate of each subplot is the number of extant species at equilibrium, out of the initial 51. Within each subplot, the three box plots correspond to different values of ω, as shown on the abscissa: they summarize the simulation results across all sets. Only results parameterized with a quadratic intrinsic growth function $b(z)$ are shown; see Supporting Information, Section 4.3 for results with a rectangular and triangular $b(z)$, yielding qualitatively the same results. Box plot guide: median (lines), 25% to 75% quartiles (boxes), ranges (whiskers), outliers (points; defined as falling outside 1.5 times the interquartile range of the box).

Notice that, while there is an important distinction between zero and nonzero heritability, the precise value of h^2 does not matter much. This can be understood from the general equations Eqs. (2) and (3): heritability multiplies the whole right hand side of Eq. (3), therefore as long as $h_i^2 \equiv h^2$ for all species, its role is simply to change the timescale of evolution.

Our simulation results are supported by an analytical derivation in the special case of $h^2 = 0$ and $\sigma_i = \sigma$ for all species. In this case, the ratio of species richnesses with- and without intraspecific variation is shown

to be

$$\frac{\text{species richness with } \sigma_i = \sigma}{\text{species richness with } \sigma_i = 0} = \frac{1}{\sqrt{4(\sigma/\omega)^2 + 1}} \tag{9}$$

(Supporting Information, Section 4.1), predicting a monotonic decline of diversity with increasing phenotypic variance. This is consistent with the results in the first row of Figure 4.

4.4 Trait patterns and detectability

Lotka–Volterra models supported the principle that coexisting species cannot be arbitrarily similar to one another (limiting similarity; MacArthur and Levins 1967). Subsequent investigations rigorously demonstrated that the likelihood of coexistence decreases with increasing species similarity (Gyllenberg and Meszéna 2005, Barabás et al. 2012), and simulation results generally support the idea that species are distributed more evenly along the trait axis than expected by chance, though this claim is not strictly proven. Here we ask how intraspecific variation affects this tendency towards even spacing.

To assess whether species' mean traits are more evenly distributed than expected by chance alone, we use the coefficient of variation (CV) of distances between the trait means of adjacent species on the trait axis; lower values indicate more even spacing. Figure 5 (left panel) shows the distribution of CVs in our simulations. Compared with the case without intraspecific variation, communities with variation tend to have lower CVs, suggesting that species are more evenly spaced when intraspecific variation occurs. However, the trend toward lower CVs with intraspecific variation is weak when heritability is zero, as can be seen by comparing the subplots of the top row. In contrast, the drop in CV is dramatic when heritability is nonzero. This suggests that when heritability is zero, even spacing is limited by the trait values available in the species pool, but this constraint is alleviated when species can evolve and thus change their initial—possibly unfavorable—trait positions.

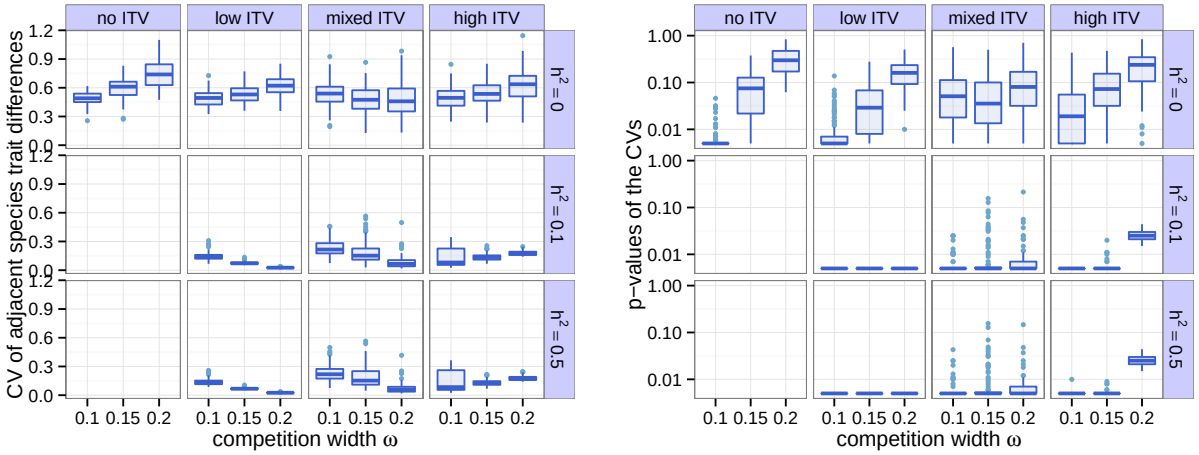

Figure 5: Left: as Figure 4, except the ordinate shows the evenness of the distribution of mean trait values along the trait axis, as measured by the coefficient of variation of nearest-neighbor distances. The CV is not changed much by nonheritable intraspecific variation, but drops significantly when heritability is nonzero. This means that the mean traits in communities where species can evolve are much more evenly spaced than in corresponding communities without the possibility of trait evolution. Right: As on the left, except the ordinate shows the probability that the degree of even spacing a given community ends up with is produced by chance (p-value). For lower values of intraspecific variability (second and third columns), heritable variation results in far lower p-values. For high levels of intraspecific variation and ω large, the effect of heritable variation on the p-values is smaller.

One may wonder whether the possibility of trait convergence described in Section 3 is realized in multispecies communities with $h^2 > 0$, and whether this would have an impact on community pattern. As it happens, such convergence is indeed observed, but too sporadically to have an appreciable impact on community structure overall (Supporting Information, Section 4.4).

Statistically significant overdispersion is commonly taken as evidence of competition structuring the community (Kraft et al. 2008, Kraft and Ackerly 2010, Baraloto et al. 2012, Vergnon et al. 2013). While one must be careful with overly simplistic applications of this idea (see, e.g., Mayfield and Levine 2010 and D'Andrea and Ostling in press), it is nevertheless meaningful to ask whether the CVs we obtained are indeed lower than expected by chance. To examine the statistical significance of the overdispersion shown in the left panel of Figure 5, we used a null model consisting of communities whose species' trait values are randomly drawn from a uniform distribution. Our null CV is independent of trait range but depends on the number of species, so each community in our data is compared to null communities of matching species richness. We compare each community in our data to a set of 1000 corresponding null communities, and obtain a p-value by tallying the proportion of null CVs that were lower than the CV in the data community. Low p-values mean the community is more evenly spaced than expected by chance. The distribution of p-values is shown in the right panel of Figure 5.

We see that significance in the cases without intraspecific variation may be high or low depending on the competition width ω. Intraspecific variation without heritability either does not substantially alter p-values ($\omega = 0.15$, 0.2), or else increases them ($\omega = 0.1$). Again, positive heritability is the real game changer, substantially lowering p-values. Overall, spacing is more even than expected by chance when species are allowed to evolve, and intraspecific variability and ω are not too large. However, these higher p-values are actually related to the fact that higher levels of variation and larger values of ω result in lower species richness (compare Figures 4 and 5), reducing statistical power. Thus p-values are increased despite the fact that spacing is more even than in corresponding cases without intraspecific variability.

We conclude that intraspecific variation by itself does not fundamentally change the original tendency for even spacing, but that this even spacing is greatly enhanced when intraspecific variation is heritable. This also greatly increases our ability to detect such spacing, except possibly when species richness is very low. This has implications for pattern detection in field studies: in communities with heritable intraspecific variation and enough species to justify pattern-based tests in the first place, species' mean traits should be significantly more evenly spaced than expected by chance.

4.5 Community robustness

Natural communities are subject to constant perturbations of abundances as well as of the environmental conditions influencing their dynamics. While reaching an eco-evolutionary equilibrium state implies its local stability, one may also ask whether it is robust—i.e., how much the community's ecological stability and feasibility are threatened by changes in the external environment (Section 3). For instance, changes in resource supply or ambient temperature may alter the shape of the growth function $b(z)$. Local stability of the community in the final state is guaranteed if the community matrix has all eigenvalues lying in the left half of the complex plane. In turn, the geometric mean of the magnitudes of the community matrix's eigenvalues is a measure of community robustness (Meszéna et al. 2006, Barabás et al. 2012, Aufderheide et al. 2013, Barabás et al. 2014) comparable across communities with different numbers of species (Supporting Information, Section 4.2). This quantity, the "average community robustness", measures the expected response of a system to perturbing environmental conditions. The left panel of Figure 6 compares this metric across our simulation sets. Intraspecific variation, in and of itself, does not influence average community robustness much. However, when heritability is nonzero, there is a strong immediate effect: communities become much more robust than they were in the absence of heritable variation. Note that this effect is not due to heritability *per se*, since two communities with the same trait distributions have equal robustness, regardless of h^2. Rather,

it is a consequence of species evolving their trait means to locations more conducive to robustness (Figure 3, middle versus right column).

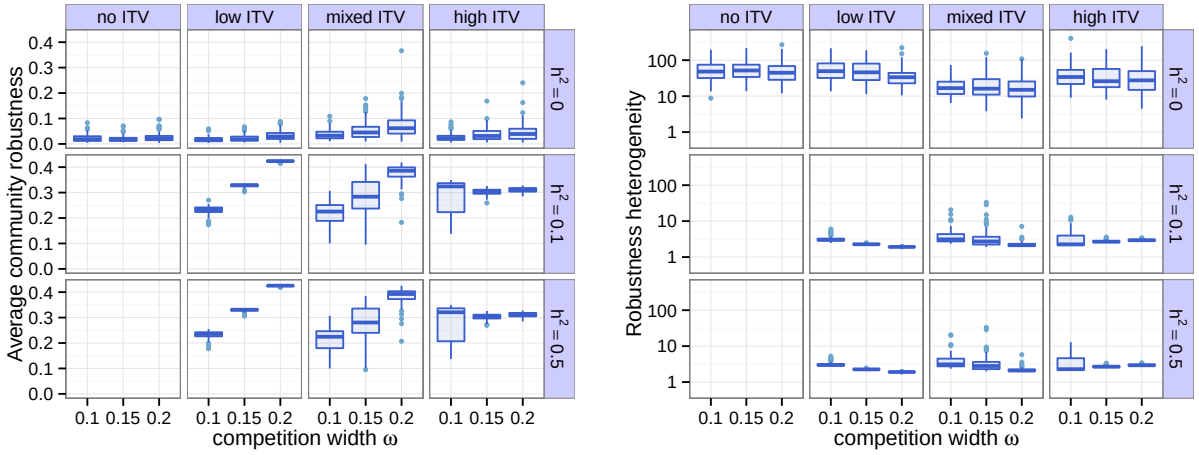

Figure 6: Left: average community robustness of our simulated communities, as measured by the geometric mean of the eigenvalues of the community matrix. Right: robustness heterogeneity of the communities, measured by the geometric standard deviation of the eigenvalues. Otherwise, the plots are organized as in Figure 4. Intraspecific variation by itself has limited effect on robustness. However, when heritability is nonzero, communities end up with both a larger average community robustness and a reduced robustness heterogeneity. This makes them far more resistant against external perturbations as a whole.

There is another aspect to robustness. Imagine two systems having identical average community robustness, but suppose the first of these reacts to every environmental perturbation in the same way, while the second one is completely insensitive to perturbing some environmental conditions, but extremely sensitive to perturbing others. It is therefore also of interest to see not just how robust a system is to the average environmental perturbation, but whether it reacts strongly to specific perturbations. This can be measured by the geometric standard deviation of the eigenvalues' magnitudes ("robustness heterogeneity"; Supporting Information, Section 4.2).

As it turns out, not only do communities with heritable variation have a higher average community robustness: their robustness heterogeneity is also much lower (Figure 6, right panel). As discussed in Section 4.4, when species can evolve, they space themselves out far more evenly along the trait axis than expected by chance. When heritability is zero however, communities sometimes end up with species very closely packed along the trait axis, with minimal niche differentiation between them and no ability to change the unfavorable trait positions, making it more likely that any particular change in environmental conditions giving an advantage to just one of those two species will result in the extinction of the other. This in turn leads to increased robustness heterogeneity.

4.6 Sensitivity of the results to the assumption of infinitely many loci

Since our model is based on quantitative genetic assumptions of an infinite number of loci contributing to the trait of interest, all trait distributions are normal, and their variances do not change in response to selection (Bulmer 1980). To check the sensitivity of our results to this assumption, we implemented finite-locus genetics using a hypergeometric model of inheritance (Shpak and Kondrashov 1999). In this case heritabilities themselves evolve, and trait distributions are no longer normal or of constant shape. We found

that even with a small number of loci, results from the finite-locus model are not qualitatively different (Supporting Information, Section 5). These assumptions are therefore not restrictive.

5 Discussion

In this work we explored the consequences of intraspecific trait variation for the stability, feasibility, and robustness of coexistence in two-species communities, and for species richness, community pattern, and robustness in multispecies communities, where individuals vary in a unidimensional trait of interest. We found that, although intraspecific variation in principle allows for coexistence between two species with more similar trait means than would be possible in the absence of such variation, species richness decreases with increasing intraspecific variance in the multispecies case. Surprisingly, trait spacing and robustness were not much affected by intraspecific variation alone. Contrary to the idea that large levels of intraspecific variation signal its ecological importance (Albert et al. 2011, Siefert et al. 2015), this suggests that nonheritable variation within a species may be safely ignored even when it is substantial, at least for the purposes of these two community properties. However, the picture changes drastically when the variation is partially heritable: species in the community become more evenly spaced along the trait axis, and more resistant to environmental perturbations.

It is common to encounter claims in the literature that intraspecific variation promotes coexistence (Hubbell 2005, Vellend 2006, Messier et al. 2010, Bolnick et al. 2011, Violle et al. 2012). Our results make a point of the importance of defining precisely what is meant by "promote". Intraspecific variation does not, for example, lead to higher species richness; rather, it always and predictably reduces species richness. On the other hand, it may lead to coexistence that is more resilient to environmental perturbations. Whether it does so depends on whether it is heritable: communities with heritable intraspecific variation evolve to a much more robust state than those without, or with nonheritable variation.

Here we have worked with supersaturated communities where the initial number of species is always substantially greater than in the final state. This means that our methods can be used to study community assembly and response to selective pressure, but are ill-suited for approaching the problem from the other end: starting with low diversity and ending up with species-rich assemblages via adaptive diversification (Geritz et al. 1998). Our model does not allow for evolutionary branching because the shape of the trait distribution cannot change in response to selection. Speciation and its effects on community structure are therefore outside our scope.

Our work is relevant for empirical studies detecting the signature of species interactions in functional trait data (Kraft et al. 2008, Kraft and Ackerly 2010, Baraloto et al. 2012, Vergnon et al. 2013). Pattern detection in these studies generally proceeds by rejecting appropriate null models assuming no interactions; significant overdispersion in the trait of interest is taken as evidence of competition structuring the community (Kraft and Ackerly 2010)—though, as mentioned before, such evidence must be interpreted with care (Mayfield and Levine 2010, D'Andrea and Ostling in press). These studies usually ignore individual variation (but see Siefert 2012). Here we took this variation into account, and also checked the sensitivity of our results to varying parameters and assumptions: different levels of intraspecific variation, shapes of the intrinsic growth function, competition widths, and heritability. The degree of intraspecific variation and the competition width have the strongest influence on species richness; positive heritability greatly enhances even spacing and robustness, and the degree of heritability affects the time scale over which these effects are observed. We also checked that our results are not sensitive to the infinite-locus assumption of quantitative genetics. All in all, the predicted community pattern is robust and very characteristic (Figure 3, right column).

Despite this strong prediction, trait data are idiosyncratic, sometimes conforming to these expectations (e.g., Grant et al. 1985), but often revealing considerable overlap between species (Clark 2010, Clark et al. 2011, Siefert 2012, Vergnon et al. 2013, Siefert et al. 2015), and no strikingly even spacing even in cases

where overdispersion is detected (e.g., Kraft et al. 2008). Discrepancy with observations may be due to a number of reasons. First, zero heritability leads to more noisy patterns (Figure 3, middle column). Second, the Lotka–Volterra model may not be adequate. Third, even if it is, competition between individuals may not be a function of their trait distance or depend on the trait at all. Fourth, immigration from outside sources may lead to persistence of species that would otherwise be extirpated. Fifth, the system could be far from equilibrium. Sixth, more than one trait could be driving community dynamics. Let us consider each of these possibilities in turn.

Studies show that almost all traits imaginable have heritabilities between 0.1 and 0.9 (Mousseau and Roff 1987), and so $h^2 = 0$ does not appear plausible—still, this must be determined empirically on a case-by-case basis. Non-Lotka–Volterra interactions (nonlinear relationships between densities and per capita growth rates) may cause the system to no longer settle on a point equilibrium: eco-evolutionary cycles (as in Vasseur et al. 2011 or Patel and Schreiber 2016) become possible. When the dynamics do settle on a point equilibrium however, linearization around the equilibrium will reduce the model to Lotka–Volterra form, and thus we do not expect fundamentally different results. Naturally, in many cases $a(z,z')$ will not be a simple function of distance, as e.g. in systems with competitive hierarchies (Tilman 1994, Muller-Landau 2010). These models may produce patterns in which spacing between species is not homogeneous along the trait axis.

For source-sink systems, sufficiently strong immigration may blur expected pattern. Immigration rates should therefore be estimated (Abadi et al. 2010), or the scale of the study extended to make the communities closed to migration. Furthermore, a system far from equilibrium may display transient patters quite different from those expected at equilibrium (D'Andrea and Ostling in press). There are ways to infer whether transients are indeed dominating. For instance, independent evidence for fast and predictable recovery from disturbance (Clark 2010) would render transients implausible. Slow recovery times make transients more likely, and successional patterns not converging on predictable species compositions may signal ecological equivalence or alternative stable states.

Even in a system with positive heritability, fast and predictable disturbance recovery, and negligible immigration, any pattern may be obscured or even reversed (a phenomenon known as the "ecological fallacy") if niche space is high-dimensional but the data are projected on a single trait axis (Clark 2010, Clark et al. 2010, 2011). We conducted a preliminary exploration and found that, although multidimensional interactions lead to the same regular spacing as in Figure 3, this regularity is lost when the pattern is projected onto just one axis (Supporting Information, Section 6). Multidimensional niche differentiation may be evidenced by whether individual-level responses to environmental changes covary more within than between species (Clark 2010). Studies aimed at detecting trait patterning along a single dimension implicitly assume that the trait in question is of overriding importance in the system at hand.

The utility of our results lie in that, when the model assumptions are met, they provide strong predictions for community structure, and when those assumptions are not met, they narrow down the potential reasons to a handful of testable hypotheses amenable to further empirical investigations. This way, they can facilitate a deeper understanding of the ecology of natural systems.

Acknowledgements

We thank S. Allesina, J. Grilli, G. Meszéna, M. Michalska-Smith, E. Sander, S. Schreiber, and C. Stepien for discussions, and convey our special thanks to A. Ostling for helpful comments and suggestions concerning the project. Comments by J. Clark and three anonymous reviewers helped significantly improve the manuscript. G. Barabás was supported by NSF #1148867. R. D'Andrea was supported by the National Science Foundation under grant 1038678 ("Niche versus Neutral Structure in Populations and Communities"), funded by the Advancing Theory in Biology program.

References

Abadi, F., Gimenez, O., Ullrich, B., Arlettaz, R., Schaub, M., 2010. Estimation of immigration rate using integrated population models. Journal of Applied Ecology 47, 393–400.

Albert, C. H., Grassein, F., Schurr, F. M., Vieilledent, G., Violle, C., 2011. When and how should intraspecific variability be considered in trait-based plant ecology? Perspectives in Plant Ecology, Evolution and Systematics 13, 217–225.

Aufderheide, H., Rudolf, L., Gross, T., Lafferty, K. D., 2013. How to predict community responses to perturbations in the face of imperfect knowledge and network complexity. Proceedings of the Royal Society of London Series B 280, 20132355.

Barabás, G., Pásztor, L., Meszéna, G., Ostling, A., 2014. Sensitivity analysis of coexistence in ecological communities: theory and application. Ecology Letters 17, 1479–1494.

Barabás, G., Pigolotti, S., Gyllenberg, M., Dieckmann, U., Meszéna, G., 2012. Continuous coexistence or discrete species? A new review of an old question. Evolutionary Ecology Research 14, 523–554.

Baraloto, C., Hardy, O. J., Paine, C. E. T., et al., 2012. Using functional traits and phylogenetic trees to examine the assembly of tropical tree communities. Journal of Ecology 100, 690–701.

Bolnick, D. I., Amarasekare, P., Araújo, M. S., Bürger, R., Levine, J. M., Novak, M., Rudolf, V. H. W., Schreiber, S. J., Urban, M. C., Vasseur, D. A., 2011. Why intraspecific trait variation matters in community ecology. Trends in Ecology and Evolution 26, 183–192.

Bulmer, M. G., 1980. The mathematical theory of quantitative genetics. Clarendon Press, Oxford, UK.

Caswell, H., 2001. Matrix population models: Construction, analysis, and interpretation. 2nd edition. Sinauer Associates.

Clark, J. S., 2010. Individuals and the variation needed for high species diversity in forest trees. Science 327, 1129–1132.

Clark, J. S., Bell, D., Chu, C. J., et al., 2010. High-dimensional coexistence based on individual variation: a synthesis of evidence. Ecological Monographs 80, 569–608.

Clark, J. S., Bell, D. M., Hersch, M. H., et al., 2011. Individual-scale variation, species-scale differences: inference needed to understand diversity. Ecology Letters 14, 1273–1287.

D'Andrea, R., Ostling, A., in press. Challenges in linking trait patterns to niche differentiation. Oikos. URL http://dx.doi.org/10.1111/oik.02979

de Roos, A., Persson, L., 2013. Population and Community Ecology of Ontogenetic Development. Princeton University Press, Princeton, NJ, USA.

Falconer, D. S., 1981. Introduction to Quantitative Genetics. Longman, London.

Geritz, S. A. H., Kisdi, É., Meszéna, G., Metz, J. A. J., 1998. Evolutionary singular strategies and the adaptive growth and branching of evolutionary trees. Evolutionary Ecology 12, 35–57.

Grant, P. R., Abbott, I., Schluter, D., Curry, R. L., Abbott, L. K., 1985. Variation in the size and shape of darwin's finches. Biological Journal of the Linnean Society 25, 1–39.

Gyllenberg, M., Meszéna, G., 2005. On the impossibility of the coexistence of infinitely many strategies. Journal of Mathematical Biology 50, 133–160.

Hubbell, S. P., 2005. Neutral theory in community ecology and the hypothesis of functional equivalence. Functional Ecology 19, 166–172.

Hughes, A. R., Inouye, B. D., Johnson, M. T. J., Underwood, N., Vellend, M., 2008. Ecological consequences of genetic diversity. Ecology Letters 11, 609–623.

Kraft, N. J., Ackerly, D. D., 2010. Functional trait and phylogenetic tests of community assembly across spatial scales in an amazonian forest. Ecological Monographs 80, 401–422.

Kraft, N. J., Valencia, R., Ackerly, D. D., 2008. Functional traits and niche-based tree community assembly in an amazonian forest. Science 322, 580–582.

Lande, R., 1976. Natural selection and random genetic drift in phenotypic evolution. Evolution 30, 314–334.

Lichstein, J., Dushoff, J., Levin, S. A., Pacala, S. W., 2007. Intraspecific variation and species coexistence. American Naturalist 170, 807–818.

MacArthur, R. H., Levins, R., 1967. Limiting similarity, convergence, and divergence of coexisting species. American Naturalist 101 (921), 377–385.

Mayfield, M. M., Levine, J. M., 2010. Opposing effects of competitive exclusion on the phylogenetic structure of communities. Ecology Letters 13, 1085–1093.

Messier, J., McGill, B. J., Lechowicz, M. J., 2010. How do traits vary across ecological scales? A case for trait-based ecology. Ecology Letters 13, 838–848.

Meszéna, G., Gyllenberg, M., Pásztor, L., Metz, J. A. J., 2006. Competitive exclusion and limiting similarity: a unified theory. Theoretical Population Biology 69, 68–87.

Metz, J. A. J., Diekmann, O., 1986. he dynamics of physiologically structured population. Springer Verlag, Berlin, Germany.

Moll, J. D., Brown, J. S., 2008. Competition and coexistence with multiple life-history stages. American Naturalist 171, 839–843.

Mousseau, T. A., Roff, D. A., 1987. Natural selection and the heritability of fitness components. Heredity 59, 181–197.

Muller-Landau, H. C., 2010. The tolerance-fecundity trade-off and the maintenance of diversity in seed size. Proceedings of the National Academy of Sciences of the USA 107, 4242–4247.

Patel, S., Schreiber, S. J., 2016. Evolutionarily driven shifts in communities with intraguild predation. American Naturalist 186, E98–E110.

Rohr, R. P., Saavedra, S., Bascompte, J., 2014. On the structural stability of mutualistic systems. Science 345. URL dx.doi.org/10.1126/science.1253497

Roughgarden, J., 1976. Resource partitioning among competing species—a coevolutionary approach. Theoretical Population Biology 9, 388–424.

Schreiber, S. J., Bürger, R., Bolnick, D. I., 2011. The community effects of phenotypic and genetic variation within a predator population. Ecology 92, 1582–1593.

Shpak, M., Kondrashov, A. S., 1999. Applicability of the hypergeometric phenotypic model to haploid and diploid populations. Evolution 53, 600–604.

Siefert, A., 2012. Incorporating intraspecific variation in tests of trait-based community assembly. Oecologia 170, 767–775.

Siefert, A., Violle, C., Chalmandrier, L., et al., 2015. A global meta-analysis of the relative extent of intraspecific trait variation in plant communities. Ecology Letters.
URL http://dx.doi.org/10.1111/ele.12508

Slatkin, M., 1979. Frequency- and density-dependent selection on a quantitative character. Genetics 93, 755–771.

Slatkin, M., 1980. Ecological character displacement. Ecology 6, 163–177.

Taper, M. L., Case, T. J., 1985. Quantitative genetic models for the coevolution of character displacement. Ecology 66, 355–371.

Tilman, D., 1994. Competition and biodiversity in spatially structured habitats. Ecology 75, 2–16.

van Leeuwen, A., Huss, M., Gardmark, A., de Roos, A. M., 2014. Ontogenetic specialism in predators with multiple niche shifts prevents predator population recovery and establishment. Ecology 95, 2409–2422.

Vasseur, D. A., Amarasekare, P., Rudolf, V. H. W., Levine, J. M., 2011. Eco-evolutionary dynamics enable coexistence via neighbor-dependent selection. American Naturalist 178, E96–E109.

Vellend, M., 2006. The consequences of genetic diversity in competitive communities. Ecology 87, 304–311.

Vergnon, R., Leijs, R., van Nes, E. H., Scheffer, M., 2013. Repeated parallel evolution reveals limiting similarity in subterranean diving beetles. American Naturalist 182, 67–75.

Vindenes, Y., Langangen, Ø., 2015. Individual heterogeneity in life histories and eco-evolutionary dynamics. Ecology Letters 18, 417–432.

Violle, C., Enquist, B. J., McGill, B. J., et al., 2012. The return of the variance: intraspecific variability in community ecology. Trends in Ecology and Evolution 27, 244–252.

Yamauchi, A., Miki, T., 2009. Intraspecific niche flexibility facilitates species coexistence in a competitive community with a fluctuating environment. Oikos 118, 55–66.

The effect of intraspecific variation and heritability on community pattern and robustness

Supporting Information

György Barabás & Rafael D'Andrea

Contents

1 Deriving the basic quantitative genetic model

1.1 The model in discrete time

We model the dynamics of S species differing in some ecologically relevant trait z. Each individual can be described by its trait, but each species is comprised of individuals with several different trait values. The number of individuals within species i at time t is $N_i(t)$, while the distribution of traits within the species is given by the function $p_i(z,t)$. By definition, this function satisfies

$$\int p_i(z,t)\,\mathrm{d}z = 1 \tag{1.1}$$

at every moment of time t; the limits of integration encompass the whole trait axis, which for simplicity we take to go between minus and plus infinity unless otherwise noted. $N_i(t)p_i(z,t)\mathrm{d}z$ is then the population density of species i's individuals with phenotype value between z and $z+\mathrm{d}z$.

The basic setup of our dynamical model follows the classical framework from population genetics (Lande 1976, Slatkin 1979, 1980, Falconer 1981, Taper and Case 1985, 1992, Schreiber et al. 2011, Vasseur et al. 2011). Usually, these formulations work in discrete time. Here we show the derivation of the continuous-time model, building on the discrete-time version in the weak selection limit.

To do this, we first assume species with nonverlapping generations undergoing selection and then reproduction:

$$N_i(t)p_i(z,t) \xrightarrow{\text{selection}} N_i'(t)p_i'(z,t) \xrightarrow{\text{reproduction}} N_i(t+T_i)p_i(z,t+T_i), \tag{1.2}$$

where the prime denotes state after selection but before reproduction, T_i is the generation time of species i, and $W_i(\vec{N},\vec{p},z,t)$ is the absolute fitness of species i's phenotype z at time t:

$$N_i'(t)p_i'(z,t) = W_i(\vec{N},\vec{p},z,t)N_i(t)p_i(z,t). \tag{1.3}$$

Note that $W_i(\vec{N},\vec{p},z,t)$ will in general depend on the abundances and trait distributions of all interacting species (denoted by the vectors $\vec{N}$ and $\vec{p}$). Here we apply the standard sleight of hand of assuming that $W_i(\vec{N},\vec{p},z,t)$ describes both birth and death processes. In principle, the population first undergoes viability selection and then reproduction as in Eq. (1.2). Having $W_i(\vec{N},\vec{p},z,t)$ include both birth and death, it is tacitly assumed that both processes happen relative to the original $N_i(t)p_i(z,t)$, instead of births happening relative to the primed quantities. This also means that the only role of the reproduction phase is to change the trait distributions $p_i(z,t)$ but not the population densities: $N_i'(t) = N_i(t+T_i)$. However, the error made this way is negligible if the difference between $N_i(t)p_i(z,t)$ and $N_i'(t)p_i'(z,t)$ is small, which will be the case if selection is sufficiently weak. We will therefore assume we are in the weak selection limit (Bürger 2011), i.e.,

$$W_i(\vec{N},\vec{p},z,t) = 1 + s\,r_i(\vec{N},\vec{p},z,t), \tag{1.4}$$

where $s \ll 1$ is a small parameter with units of inverse time, and the function $r_i(\vec{N},\vec{p},z,t)$ is the rate of births minus deaths at time t. It is therefore the per capita growth rate of species i, determined by the ecological interactions within the community.

We work in the quantitative genetic limit, i.e., the trait in question is determined by the action of many independent loci, each contributing a small additive effect to the trait. In this case, the following important results hold (Bulmer 1980, Falconer 1981):

- The trait distribution is always normal, so one can write

$$p_i(z,t) = \sqrt{\frac{1}{2\pi\sigma_i^2}}\exp\left(-\frac{(z-\mu_i(t))^2}{2\sigma_i^2}\right), \tag{1.5}$$

  where $\mu_i(t)$ is the mean trait of species i at time t, and σ_i^2 is its intraspecific trait variance.

- Only the mean $\mu_i(t)$ changes in response to selection, leaving both the shape and the variance of $p_i(z,t)$ unaffected. This introduces a great simplification because, instead of having to track the dynamics of the whole trait distribution, we can simply track its mean and treat the σ_i^2 as externally defined parameters to the model. This simplification is the consequence of the idealization that infinitely many loci, each with an infinitesimal additive effect, determine the genetic makeup of the trait in question; see Section 5 for the effects of relaxing this assumption.
- The total phenotypic variance σ_i^2 of species i is the sum of the additive genetic variance $\sigma_{A,i}^2$ and the environmental variance $\sigma_{E,i}^2$. The ratio $h_i^2 = \sigma_{A,i}^2/(\sigma_{A,i}^2+\sigma_{E,i}^2) = \sigma_{A,i}^2/\sigma_i^2$ is the heritability of the trait. Since in the limit of quantitative genetics the additive variance does not change, and we will assume throughout that the environmental variance of a given species is also unchanging, this means that the h_i^2 remain constant as well.

With this specification of the selection and birth processes, one can derive the dynamics of the species densities and traits for any fitness function $W_i(\vec{N},\vec{p},z,t)$. To obtain the dynamics of the population densities from one generation to the next, we integrate Eq. (1.3) over z to get

$$N_i'(t)\int p_i'(z,t)\,\mathrm{d}z = N_i(t)\int W_i(\vec{N},\vec{p},z,t)p_i(z,t)\,\mathrm{d}z. \tag{1.6}$$

Using $N_i'(t) = N_i(t+T_i)$ and Eq. (1.1) on the left hand side:

$$N_i(t+T_i) = N_i(t)\int W_i(\vec{N},\vec{p},z,t)p_i(z,t)\,\mathrm{d}z. \tag{1.7}$$

To obtain the time evolution of the trait distributions, note that only their means can change in the quantitative genetics approximation, as discussed above. Therefore we only need to track $\mu_i(t)$ instead of $p_i(z,t)$. By definition, the mean trait at time t is given by

$$\mu_i(t) = \int z p_i(z,t)\,\mathrm{d}z. \tag{1.8}$$

The equation for the trait means can be written using the breeder's equation (Falconer 1981), according to which the change in mean trait from one generation to the next (response to selection) is equal to the heritability times the selection differential:

$$\mu_i(t+T_i) - \mu_i(t) = h_i^2\left[\mu_i'(t) - \mu_i(t)\right]. \tag{1.9}$$

Here h_i^2 is the heritability, and $\mu_i'(t)$ is the mean of the trait after selection but before reproduction. We can obtain $\mu_i'(t)$ by first rearranging Eq. (1.3) and using $N_i'(t) = N_i(t+T_i)$:

$$p_i'(z,t) = \frac{W_i(\vec{N},\vec{p},z,t)N_i(t)p_i(z,t)}{N_i(t+T_i)}. \tag{1.10}$$

Using Eq. (1.7) in the denominator:

$$p_i'(z,t) = \frac{W_i(\vec{N},\vec{p},z,t)N_i(t)p_i(z,t)}{N_i(t)\displaystyle\int W_i(\vec{N},\vec{p},z',t)p_i(z',t)\,\mathrm{d}z'} = \frac{W_i(\vec{N},\vec{p},z,t)p_i(z,t)}{\displaystyle\int W_i(\vec{N},\vec{p},z',t)p_i(z',t)\,\mathrm{d}z'}, \tag{1.11}$$

where we switched to z' for the integration variable to distinguish it from z in the numerator. Multiplying both sides of Eq. (1.11) by z and integrating, we get

$$\int z p_i'(z,t)\,\mathrm{d}z = \frac{\displaystyle\int z W_i(\vec{N},\vec{p},z,t)p_i(z,t)\,\mathrm{d}z}{\displaystyle\int W_i(\vec{N},\vec{p},z',t)p_i(z',t)\,\mathrm{d}z'}, \tag{1.12}$$

or, using Eq. (1.8) on the left hand side,

$$\mu_i'(t) = \frac{\int z W_i(\vec{N},\vec{p},z,t) p_i(z,t)\,\mathrm{d}z}{\int W_i(\vec{N},\vec{p},z',t) p_i(z',t)\,\mathrm{d}z'}. \tag{1.13}$$

Substituting this into the breeder's equation Eq. (1.9), we finally have

$$\mu_i(t+T_i) - \mu_i(t) = h_i^2 \left(\frac{\int z W_i(\vec{N},\vec{p},z,t) p_i(z,t)\,\mathrm{d}z}{\int W_i(\vec{N},\vec{p},z',t) p_i(z',t)\,\mathrm{d}z'} - \mu_i(t) \right). \tag{1.14}$$

1.2 Continuous-time dynamics in the weak selection limit

We can obtain a differential equation approximation to Eqs. (1.7) and (1.14) in the weak selection limit of Eq. (1.4). Starting with Eq. (1.7), it reads

$$N_i(t+T_i) = N_i(t) \int \Big[1 + s\, r_i(\vec{N},\vec{p},z,t)\Big] p_i(z,t)\,\mathrm{d}z, \tag{1.15}$$

or, using Eq. (1.1) on the right hand side,

$$N_i(t+T_i) = N_i(t) + sN_i(t) \int r_i(\vec{N},\vec{p},z,t) p_i(z,t)\,\mathrm{d}z. \tag{1.16}$$

Rearranging, we get

$$\frac{N_i(t+T_i) - N_i(t)}{s} = N_i(t) \int r_i(\vec{N},\vec{p},z,t) p_i(z,t)\,\mathrm{d}z. \tag{1.17}$$

We define the dimensionless measure of time $\tau = ts$ and the new density measure $\tilde{N}_i(\tau) = N_i(t)$ (Nagylaki 1992, p. 99; Bürger 2011). The left hand side above then reads $[\tilde{N}_i(\tau + T_i s) - \tilde{N}_i(\tau)]/s$, which in the limit of $s \to 0$ converges to $\mathrm{d}\tilde{N}_i(\tau)/\mathrm{d}\tau$. Understanding that this change of units has taken place but reverting to our original symbols t and $N_i(t)$ for notational convenience, Eq. (1.17) finally becomes

$$\frac{\mathrm{d}N_i(t)}{\mathrm{d}t} = N_i(t) \int r_i(\vec{N},\vec{p},z,t) p_i(z,t)\,\mathrm{d}z. \tag{1.18}$$

Turning to the trait means, Eq. (1.14) in the weak selection limit of Eq. (1.4) reads

$$\mu_i(t+T_i) - \mu_i(t) = h_i^2 \left(\frac{\int z \Big[1 + s\, r_i(\vec{N},\vec{p},z,t)\Big] p_i(z,t)\,\mathrm{d}z}{\int \Big[1 + s\, r_i(\vec{N},\vec{p},z',t)\Big] p_i(z',t)\,\mathrm{d}z'} - \mu_i(t) \right). \tag{1.19}$$

Using Eqs. (1.1) and (1.8) on the right hand side:

$$\mu_i(t+T_i) - \mu_i(t) = h_i^2 \left(\frac{\mu_i(t) + s\int z r_i(\vec{N},\vec{p},z,t) p_i(z,t)\,\mathrm{d}z}{1 + s\int r_i(\vec{N},\vec{p},z',t) p_i(z',t)\,\mathrm{d}z'} - \mu_i(t) \right). \tag{1.20}$$

Taylor expanding in $s \ll 1$ and neglecting terms of order s^2 or higher:

$$\mu_i(t+T_i) - \mu_i(t) \approx h_i^2 \left(s\int z r_i(\vec{N},\vec{p},z,t) p_i(z,t)\,\mathrm{d}z - \mu_i(t) s \int r_i(\vec{N},\vec{p},z,t) p_i(z,t)\,\mathrm{d}z \right). \tag{1.21}$$

Rearranging, we get

$$\frac{\mu_i(t+T_i)-\mu_i(t)}{s} = h_i^2 \int (z-\mu_i(t)) r_i(\vec{N},\vec{p},z,t) p_i(z,t)\,\mathrm{d}z, \tag{1.22}$$

at which point we can rescale time and take the $s \to 0$ limit exactly as before, obtaining

$$\frac{\mathrm{d}\mu_i(t)}{\mathrm{d}t} = h_i^2 \int (z-\mu_i(t)) r_i(\vec{N},\vec{p},z,t) p_i(z,t)\,\mathrm{d}z. \tag{1.23}$$

Eqs. (1.18) and (1.23) govern the eco-evolutionary dynamics of the community given the ecology of the system, specified by the function $r_i(\vec{N},\vec{p},z,t)$.

Although we obtained the governing differential equations in the weak selection limit, note that there are alternative ways of arriving at Eqs. (1.18) and (1.23) which do not rely on this approximation—see, e.g., Lande (1982) for a derivation which assumes that the populations are at their stable age structure. The results are therefore expected to hold even when selection is not very weak.

2 A quantitative genetic Lotka–Volterra model

2.1 Dynamical equations

The Lotka–Volterra model for S species is defined by the per capita growth rates

$$r(\vec{N},\vec{p},z,t) = b(z) - \sum_{j=1}^{S} N_j(t) \int a(z,z') p_j(z',t)\,\mathrm{d}z', \tag{2.1}$$

where $b(z)$ and $a(z,z')$ are appropriately chosen functions for the intrinsic growth rate of phenotype z and the interaction coefficient between phenotypes z and z', respectively. The summation over species and the integral across all phenotypes means that every individual with phenotype z interacts with all other individuals in the community. This particular formulation of the Lotka–Volterra model is special in the sense that growth and interactions only depend on the phenotype z but not on species identity. In other words, two individuals of two different species are exchangeable without altering the growth rates. Note that this is only true in the context of the interaction structure defined by Eq. (2.1): species identity does matter in the context of reproduction in the quantitative genetic limit, where the shape of the trait distributions must be maintained to match Eq. (1.5).

We can substitute Eq. (2.1) into Eqs. (1.18) and (1.23) to obtain the dynamics. Starting with Eq. (1.18), we have

$$\begin{aligned} \frac{\mathrm{d}N_i(t)}{\mathrm{d}t} &= N_i(t) \int r_i(\vec{N},\vec{p},z,t) p_i(z,t)\,\mathrm{d}z \\ &= N_i(t) \int p_i(z,t) \left(b(z) - \sum_{j=1}^{S} N_j(t) \int a(z,z') p_j(z',t)\,\mathrm{d}z' \right) \mathrm{d}z. \end{aligned} \tag{2.2}$$

Introducing the notation

$$b_i(t) = \int p_i(z,t) b(z)\,\mathrm{d}z, \tag{2.3}$$

$$\alpha_{ij}(t) = \iint p_i(z,t) a(z,z') p_j(z',t)\,\mathrm{d}z'\mathrm{d}z, \tag{2.4}$$

we can write

$$\begin{aligned}\frac{\mathrm{d}N_i(t)}{\mathrm{d}t} &= N_i(t)\left(\underbrace{\int p_i(z,t)b(z)\,\mathrm{d}z}_{b_i(t)} - \sum_{j=1}^{S} N_j(t)\underbrace{\iint p_i(z,t)a(z,z')p_j(z',t)\,\mathrm{d}z'\mathrm{d}z}_{\alpha_{ij}(t)}\right)\\ &= N_i(t)\left(b_i(t) - \sum_{j=1}^{S}\alpha_{ij}(t)N_j(t)\right).\end{aligned} \tag{2.5}$$

The interpretation of $b_i(t)$ is the population-level intrinsic growth rate of species i, while $\alpha_{ij}(t)$ is the population-level competitive effect of species j on species i.

Similarly, Eq. (1.23) will read

$$\begin{aligned}\frac{\mathrm{d}\mu_i(t)}{\mathrm{d}t} &= h_i^2\int (z-\mu_i(t))r_i(\vec{N},\vec{p},z,t)p_i(z,t)\,\mathrm{d}z\\ &= h_i^2\int (z-\mu_i(t))p_i(z,t)\left(b(z) - \sum_{j=1}^{S}N_j(t)\int a(z,z')p_j(z',t)\,\mathrm{d}z'\right)\mathrm{d}z.\end{aligned} \tag{2.6}$$

Again, after introducing

$$\overline{b}_i(t) = \int (z-\mu_i(t))p_i(z,t)b(z)\,\mathrm{d}z, \tag{2.7}$$

$$\beta_{ij}(t) = \iint (z-\mu_i(t))p_i(z,t)a(z,z')p_j(z',t)\,\mathrm{d}z'\mathrm{d}z, \tag{2.8}$$

we get

$$\begin{aligned}\frac{\mathrm{d}\mu_i(t)}{\mathrm{d}t} &= h_i^2\underbrace{\int (z-\mu_i(t))p_i(z,t)b(z)\,\mathrm{d}z}_{\overline{b}_i(t)} - h_i^2\sum_{j=1}^{S}N_j(t)\underbrace{\iint (z-\mu_i(t))p_i(z,t)a(z,z')p_j(z',t)\,\mathrm{d}z'\mathrm{d}z}_{\beta_{ij}(t)}\\ &= h_i^2\left(\overline{b}_i(t) - \sum_{j=1}^{S}\beta_{ij}(t)N_j(t)\right).\end{aligned} \tag{2.9}$$

Here $\overline{b}_i(t)$ quantifies the selective pressure on the trait mean of species i caused by growth, and $\beta_{ij}(t)$ the selective pressure on the trait mean of species i caused by competition with species j.

Writing out the final results, the following system of differential equations describes the eco-evolutionary dynamics under Lotka–Volterra competition in the quantitative genetic limit:

$$\frac{\mathrm{d}N_i(t)}{\mathrm{d}t} = N_i(t)\left(b_i(t) - \sum_{j=1}^{S}\alpha_{ij}(t)N_j(t)\right), \tag{2.10}$$

$$\frac{\mathrm{d}\mu_i(t)}{\mathrm{d}t} = h_i^2\left(\overline{b}_i(t) - \sum_{j=1}^{S}\beta_{ij}(t)N_j(t)\right). \tag{2.11}$$

2.2 The Jacobian of the quantitative genetic Lotka–Volterra model

The Jacobian of the dynamical equations Eqs. (2.10) and (2.11) is

$$J_{ik} = \frac{\partial\left(\frac{\mathrm{d}N_i}{\mathrm{d}t}, \frac{\mathrm{d}\mu_i}{\mathrm{d}t}\right)}{\partial(N_k, \mu_k)}. \tag{2.12}$$

We can calculate its entries block-by-block:

$$\begin{aligned}
\frac{\partial(\mathrm{d}N_i/\mathrm{d}t)}{\partial N_k} &= \delta_{ik}\left(b_i - \sum_{j=1}^{S}\alpha_{ij}N_j\right) - N_i\alpha_{ik},\\
\frac{\partial(\mathrm{d}N_i/\mathrm{d}t)}{\partial \mu_k} &= N_i\left(\frac{\partial b_i}{\partial \mu_k} - \sum_{j=1}^{S}\frac{\partial \alpha_{ij}}{\partial \mu_k}N_j\right) = N_i\left(\frac{\partial b_i}{\partial \mu_k}\delta_{ik} - \sum_{j\neq i}^{S}\left(\delta_{ik}+\delta_{jk}\right)\frac{\partial \alpha_{ij}}{\partial \mu_k}N_j\right),\\
\frac{\partial(\mathrm{d}\mu_i/\mathrm{d}t)}{\partial N_k} &= -h_i^2\beta_{ik},\\
\frac{\partial(\mathrm{d}\mu_i/\mathrm{d}t)}{\partial \mu_k} &= h_i^2\left(\frac{\partial \bar{b}_i}{\partial \mu_k} - \sum_{j=1}^{S}\frac{\partial \beta_{ij}}{\partial \mu_k}N_j\right) = h_i^2\left(\frac{\partial \bar{b}_i}{\partial \mu_k}\delta_{ik} - \sum_{j=1}^{S}\left(\delta_{ik}+\delta_{jk}\right)\frac{\partial \beta_{ij}}{\partial \mu_k}N_j\right),
\end{aligned} \tag{2.13}$$

where δ_{ij} is the Kronecker symbol, equal to 1 if $i=j$ and to 0 otherwise. Here we used the fact that b_i and $\bar{b}_i$ only depend on μ_i but not on $\mu_{k\neq i}$; similarly, α_{ij} and β_{ij} only depend on μ_i and μ_j but not on $\mu_{k\neq i,j}$.

Collecting everything in a block-matrix, we get

$$J_{ik} = \begin{pmatrix} \delta_{ik}\left(b_i - \sum_{j=1}^{S}\alpha_{ij}N_j\right) - N_i\alpha_{ik} & N_i\left(\frac{\partial b_i}{\partial \mu_k}\delta_{ik} - \sum_{j\neq i}^{S}\left(\delta_{ik}+\delta_{jk}\right)\frac{\partial \alpha_{ij}}{\partial \mu_k}N_j\right) \\ -h_i^2\beta_{ik} & h_i^2\left(\frac{\partial \bar{b}_i}{\partial \mu_k}\delta_{ik} - \sum_{j=1}^{S}\left(\delta_{ik}+\delta_{jk}\right)\frac{\partial \beta_{ij}}{\partial \mu_k}N_j\right)\end{pmatrix}. \tag{2.14}$$

For S coexisting species, the equilibrium condition for the abundances can be expressed from Eq. (2.10) as the solution to

$$b_i = \sum_{j=1}^{S}\alpha_{ij}\hat{N}_j, \tag{2.15}$$

where the hat denotes equilibrium values. When evaluating the Jacobian at this equilibrium, the first term of the top left block cancels and we are left with

$$\left.\frac{\partial(\mathrm{d}N_i/\mathrm{d}t)}{\partial N_k}\right|_{\hat{N}} = -\hat{N}_i\alpha_{ik}. \tag{2.16}$$

This is the community matrix (Levins 1968, May 1973), which we will denote with M:

$$M_{ik} = -\hat{N}_i\alpha_{ik}. \tag{2.17}$$

2.3 Parameterizing the quantitative genetic Lotka–Volterra model

In this section, we choose the functional forms of the quantitative genetic Lotka–Volterra model's ingredient functions in three alternative ways. First, as a common point across all three parameterizations, we choose a Gaussian interaction kernel that depends only on trait difference and not on the actual trait values themselves (homogeneous function):

$$a(z,z') = \exp\left(-\frac{(z-z')^2}{\omega^2}\right). \tag{2.18}$$

Here ω determines the width of the kernel. We can now calculate $\alpha_{ij}(t)$ and $\beta_{ij}(t)$ by direct integration, using Eqs. (2.4) and (2.8):

$$\alpha_{ij}(t) = \frac{\omega}{\sqrt{2\sigma_i^2 + 2\sigma_j^2 + \omega^2}} \exp\left(-\frac{(\mu_i(t) - \mu_j(t))^2}{2\sigma_i^2 + 2\sigma_j^2 + \omega^2} \right), \tag{2.19}$$

$$\beta_{ij}(t) = -\frac{2\omega\sigma_i^2(\mu_i(t) - \mu_j(t))}{\left(2\sigma_i^2 + 2\sigma_j^2 + \omega^2\right)^{3/2}} \exp\left(-\frac{(\mu_i(t) - \mu_j(t))^2}{2\sigma_i^2 + 2\sigma_j^2 + \omega^2} \right). \tag{2.20}$$

For $b(z)$, we use three alternative forms, each expressing different biological scenarios.

I. $b(z)$ rectangular:

$$b(z) = \begin{cases} 1 & \text{if } -\theta \le z \le \theta, \\ 0 & \text{otherwise.} \end{cases} \tag{2.21}$$

This function equals one in $[-\theta, \theta]$ and zero outside. Therefore, an individual with phenotype z can thrive equally efficiently within those limits but is suddenly unable to thrive at all outside. With $b(z)$ specified, the integrals for $b_i(t)$ and $\bar{b}_i(t)$, given in Eqs. (2.3) and (2.7), evaluate to

$$b_i(t) = \frac{1}{2}\left[\operatorname{erf}\left(\frac{\theta - \mu_i(t)}{\sqrt{2}\sigma_i} \right) + \operatorname{erf}\left(\frac{\theta + \mu_i(t)}{\sqrt{2}\sigma_i} \right) \right], \tag{2.22}$$

$$\bar{b}_i(t) = \frac{\sigma_i}{\sqrt{2\pi}} \exp\left(-\frac{(\theta + \mu_i(t))^2}{2\sigma_i^2} \right) \left[1 - \exp\left(\frac{2\theta\mu_i(t)}{\sigma_i^2} \right) \right]. \tag{2.23}$$

II. $b(z)$ quadratic:

$$b(z) = \begin{cases} 1 - z^2/\theta^2 & \text{if } -\theta \le z \le \theta, \\ 0 & \text{otherwise.} \end{cases} \tag{2.24}$$

This function decreases quadratically from its maximum at $z = 0$ and becomes zero at $z = \pm\theta$. This means that there is a tradeoff between trait magnitude and performance: more extreme trait values have lower growth rates. Integrating for $b_i(t)$ and $\bar{b}_i(t)$ using Eqs. (2.3) and (2.7), we get

$$\begin{aligned} b_i(t) = \frac{1}{2\theta^2} \exp\left(-\frac{\theta^2 + \mu_i^2(t)}{\sigma_i^2} \right) \Bigg\{ & \exp\left(\frac{\theta^2 + \mu_i^2(t)}{\sigma_i^2} \right) \left(\theta^2 - \sigma_i^2 - \mu_i^2(t) \right) \\ & \times \left[\operatorname{erf}\left(\frac{\theta - \mu_i(t)}{\sqrt{2}\sigma_i} \right) + \operatorname{erf}\left(\frac{\theta + \mu_i(t)}{\sqrt{2}\sigma_i} \right) \right] \\ & + \sqrt{\frac{2}{\pi}}\sigma_i \exp\left(\frac{(\theta - \mu_i(t))^2}{2\sigma_i^2} \right) \left[\theta + (\theta + \mu_i(t)) \exp\left(\frac{2\theta\mu_i(t)}{\sigma_i^2} \right) - \mu_i(t) \right] \Bigg\}, \end{aligned} \tag{2.25}$$

$$\begin{aligned} \bar{b}_i(t) = -\frac{\sigma_i^2}{\theta^2} \exp\left(-\frac{\theta^2 + \mu_i^2(t)}{\sigma_i^2} \right) \Bigg\{ & \mu_i(t) \exp\left(\frac{\theta^2 + \mu_i^2(t)}{\sigma_i^2} \right) \\ & \times \left[\operatorname{erf}\left(\frac{\theta - \mu_i(t)}{\sqrt{2}\sigma_i} \right) + \operatorname{erf}\left(\frac{\theta + \mu_i(t)}{\sqrt{2}\sigma_i} \right) \right] \\ & + \sqrt{\frac{2}{\pi}}\sigma_i \left[\exp\left(\frac{(\theta - \mu_i(t))^2}{2\sigma_i^2} \right) - \exp\left(\frac{(\theta + \mu_i(t))^2}{2\sigma_i^2} \right) \right] \Bigg\}. \end{aligned} \tag{2.26}$$

III. $b(z)$ triangular:

$$b(z) = \begin{cases} \dfrac{z+\theta}{2\theta} & \text{if } -\theta \le z \le \theta, \\ 0 & \text{otherwise.} \end{cases} \tag{2.27}$$

This function increases linearly from zero to one in the interval $[-\theta, \theta]$ and is zero outside. As in the quadratic case, there is a tradeoff between trait value and performance, but it is asymmetric: smaller trait values are always less viable than larger ones in the region $[-\theta, \theta]$. Using Eqs. (2.3) and (2.7), $b_i(t)$ and $\overline{b}_i(t)$ evaluate to

$$\begin{aligned} b_i(t) = {} & \frac{\theta+\mu_i(t)}{4\theta}\left[\operatorname{erf}\left(\frac{\theta-\mu_i(t)}{\sqrt{2}\sigma_i}\right)+\operatorname{erf}\left(\frac{\theta+\mu_i(t)}{\sqrt{2}\sigma_i}\right)\right] \\ & -\frac{\sigma_i}{4\theta}\sqrt{\frac{2}{\pi}}\exp\left(-\frac{(\theta+\mu_i(t))^2}{2\sigma_i^2}\right)\left[\exp\left(\frac{2\theta\mu_i(t)}{\sigma_i^2}\right)-1\right], \end{aligned} \tag{2.28}$$

$$\overline{b}_i(t) = \frac{\sigma_i^2}{4\theta}\left[\operatorname{erf}\left(\frac{\theta-\mu_i(t)}{\sqrt{2}\sigma_i}\right)+\operatorname{erf}\left(\frac{\theta+\mu_i(t)}{\sqrt{2}\sigma_i}\right)\right]-\frac{\sigma_i}{\sqrt{2\pi}}\exp\left(-\frac{(\theta-\mu_i(t))^2}{2\sigma_i^2}\right). \tag{2.29}$$

Substituting the results of either parameterization into Eqs. (2.10) and (2.11), the model is fully specified up to choosing numerical values for the parameters.

3 Two-species results

Here we use the quantitative genetic Lotka–Volterra model as described above in Section 2, except we do not specify $b(z)$ in any particular way unless noted otherwise. We set the number of species S to two.

3.1 The ecological equilibrium and its stability

Let us consider just the ecological part of the dynamics. The equilibrium condition is given by setting Eq. (2.10) to zero. Requiring that the equilibrium densities be nonzero, we have, for $S = 2$,

$$b_i = \sum_{j=1}^{2} \alpha_{ij}\hat{N}_j, \tag{3.1}$$

where the hat denotes equilibrium values. The solution for the $\hat{N}_i$ is obtained by multiplying both sides with the inverse of the matrix α_{ij}:

$$\hat{N}_i = \sum_{j=1}^{2} \left(\alpha^{-1}\right)_{ij} b_j. \tag{3.2}$$

Assuming that the equilibrium described by Eq.(3.2) is feasible (i.e., all equilibrium abundances are positive), its global stability can be established. Writing out α_{ij} using Eq. (2.19), we get

$$\alpha_{ij} = \omega \begin{pmatrix} \dfrac{1}{\sqrt{4\sigma_1^2+\omega^2}} & \dfrac{\exp\left(-d^2\left(2\sigma_1^2+2\sigma_2^2+\omega^2\right)^{-1}\right)}{\sqrt{2\sigma_1^2+2\sigma_2^2+\omega^2}} \\ \dfrac{\exp\left(-d^2\left(2\sigma_1^2+2\sigma_2^2+\omega^2\right)^{-1}\right)}{\sqrt{2\sigma_1^2+2\sigma_2^2+\omega^2}} & \dfrac{1}{\sqrt{4\sigma_2^2+\omega^2}} \end{pmatrix}, \tag{3.3}$$

where $d = |\mu_1 - \mu_2|$ is the distance between the species' mean traits. This matrix is symmetric (implying that both eigenvalues are real), and purely competitive. Then, due to the classic theorem of MacArthur (1970), global stability of the equilibrium Eq. (3.2), if it exists, is guaranteed as long as $-\alpha_{ij}$ has strictly negative eigenvalues. This in turn will hold if the trace and determinant of $-\alpha_{ij}$ are negative and positive, respectively (Routh–Hurwitz criteria; Edelstein-Keshet 1988). The trace of $-\alpha_{ij}$ is trivially negative. To show that the determinant $\Delta = \det(-\alpha_{ij}) = (-1)^2 \det(\alpha_{ij}) = \det(\alpha_{ij})$ is positive, we calculate it using Eq. (3.3):

$$\Delta = \alpha_{11}\alpha_{22} - \alpha_{12}\alpha_{21} = \omega^2 \left(\frac{1}{\sqrt{\left(4\sigma_1^2 + \omega^2\right)\left(4\sigma_2^2 + \omega^2\right)}} - \frac{\exp\left(-2d^2\left(2\sigma_1^2 + 2\sigma_2^2 + \omega^2\right)^{-1}\right)}{2\sigma_1^2 + 2\sigma_2^2 + \omega^2} \right). \tag{3.4}$$

The exponential expression in the numerator of the second term is less than or equal to one. Notice that the larger this exponent is, the smaller the determinant will be. Assuming therefore, as a worst-case scenario, that it is precisely equal to one (i.e., $d = 0$), the determinant Δ will be positive as long as the denominator of the first term is smaller than the denominator of the second:

$$\sqrt{\left(4\sigma_1^2 + \omega^2\right)\left(4\sigma_2^2 + \omega^2\right)} < 2\sigma_1^2 + 2\sigma_2^2 + \omega^2. \tag{3.5}$$

Taking the square of both sides, rearranging, and simplifying, we get $0 < \left(\sigma_1^2 - \sigma_2^2\right)^2$ as the condition for the positivity of the determinant, which is always satisfied except when $\sigma_1 = \sigma_2$. This establishes that any feasible equilibrium given by Eq. (3.2) will be globally stable unless $d = 0$ and $\sigma_1 = \sigma_2$ simultaneously.

3.2 Robustness and feasibility

The sensitivity of the equilibrium densities in Eq. (3.2) to perturbations of the b_i and α_{ij} depends on the determinant Δ. Since the $\hat{N}_i$ are proportional to the inverse of α_{ij}, and the inverse of a matrix is in turn proportional to the inverse of its determinant, a small Δ means that a large number will multiply any perturbation of the parameters, causing a sudden, large shift in the equilibrium densities, increasing the risk of extinction (Meszéna et al. 2006, Barabás et al. 2014b). We should therefore see what the effect of intraspecific variation is on the determinant of α_{ij}.

In the limit of no intraspecific variation ($\sigma_1 = \sigma_2 = 0$), the determinant in Eq. (3.4) reduces to

$$\Delta_0 = 1 - \exp\left(-2d^2/\omega^2\right). \tag{3.6}$$

We can compare the determinant Δ of the two-species system with that of the exact same system, except that we set σ_1 and σ_2 to zero. This is effectively a comparison of the system's robustness with- and without intraspecific variability.

Figure 1 shows both Δ_0 and Δ separately (left) as well as the ratio of Δ to Δ_0 (right) as a function of the mean trait difference d, for various values of the intraspecific variance σ_2^2. What we see is that for large d the Δ/Δ_0 ratios asymptote, at smaller values for larger levels of intraspecific variation and always below one. This means that for $d \to \infty$, intraspecific variation makes the two-species system more sensitive to parameter perturbations than it would be in the absence of such variation. This can be understood in the following way: as the distance between the species grows very large, the interspecific species interactions become negligible. Indeed, from Eq. (3.3) we see that α_{12} and α_{21} approach zero as $d \to \infty$. Then, the two species decouple into two independent species following logistic growth, whose sensitivity depends on the strength of their intraspecific interactions α_{11} and α_{22}: the stronger the self-regulation, the smaller the sensitivity due to an increased determinant. Again, from Eq. (3.3) we see that the diagonal terms get smaller with increasing σ_1 and σ_2. Intuitively, this is because for σ_i small, all individuals have the same phenotype and

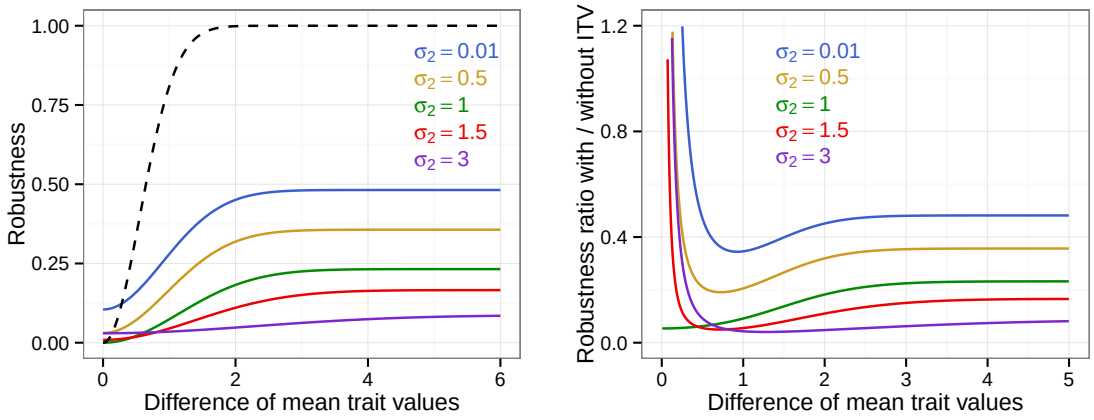

Figure 1: The dependence of robustness on mean trait distance and intraspecific variability. For all curves, $\omega = 1.1$. For all curves except the black dashed line on the left, $\sigma_1 = 1$. Left: robustness, as measured by $\Delta = \det(\alpha_{ij})$. The dashed black line is the reference case with no intraspecific variation: $\sigma_1 = \sigma_2 = 0$. For all solid curves, $\sigma_1 = 1$ and colors denote different values of σ_2 (see legend). Except for very small differences in mean trait, the case with no intraspecific variation leads to the greatest robustness. Intraspecific variation therefore promotes the coexistence of tightly packed species, but only if their σs are sufficiently different. Right: the ratio of the determinants with- and without intraspecific variation, Δ/Δ_0 The ratio is approximately constant but lower than one for d large, decreases slightly for d commensurable with the intraspecific standard deviations, and approaches infinity as $d \to 0$.

therefore compete strongly, whereas for σ_i large, different individuals of the same species avoid competition by sufficiently differing in their phenotypes.

In contrast, as d approaches zero, Δ/Δ_0 goes to infinity except when $\sigma_1 = \sigma_2$. Mathematically, this is because Δ_0 always approaches zero as $d \to 0$, but Δ will only do so if $\sigma_1 = \sigma_2$. This can be understood in terms of Figure 2. If the variances of the two species differ (left), the species with the higher variance will have nonoverlapping individuals with the other species, thus reducing interspecific competition—a phenomenon known as phenotypic subsidy (Bolnick et al. 2011). But if there is no variation or the two variances are very similar (right), the two species compete maximally. On the left, the yellow species is a generalist while the blue species is a specialist; this arrangement allows for stable coexistence despite the fact that the two trait means precisely coincide.

The final interesting aspect of Figure 1 is that the determinant ratio Δ/Δ_0 does not vary monotonically with d, but instead has a minimum at some intermediate distance (except when $\sigma_1 = \sigma_2$). At this distance, some individuals are completely overlapping in their traits, and some are farther away than expected based on the mean trait alone. However, due to the nonlinear dependence of competition on trait distance (Eq. 2.18, Figure 2), overlapping individuals have a greater impact on coexistence than distant ones. This effect disappears when the distance gets so large that there is no longer any appreciable trait overlap between heterospecific individuals.

In summary, the sensitivity of coexistence to parameter perturbations is in general heightened by intraspecific variation, except when the mean traits of the two species are very close. In that case, stable and robust coexistence is possible even when the mean traits are identical ($d = 0$).

There is an alternative way of characterizing the robustness of coexistence and its dependence on intraspecific variation. We could ask: for two species with given trait means and variances, what is the fraction of different growth rate vectors (b_1, b_2) out of all possible combinations leading to a stable and feasible (all-positive) equilibrium? Since it was established in Section 3.1 that any feasible equilibrium will automatically be globally stable, we can concentrate just on feasibility. First, note that in Lotka–Volterra

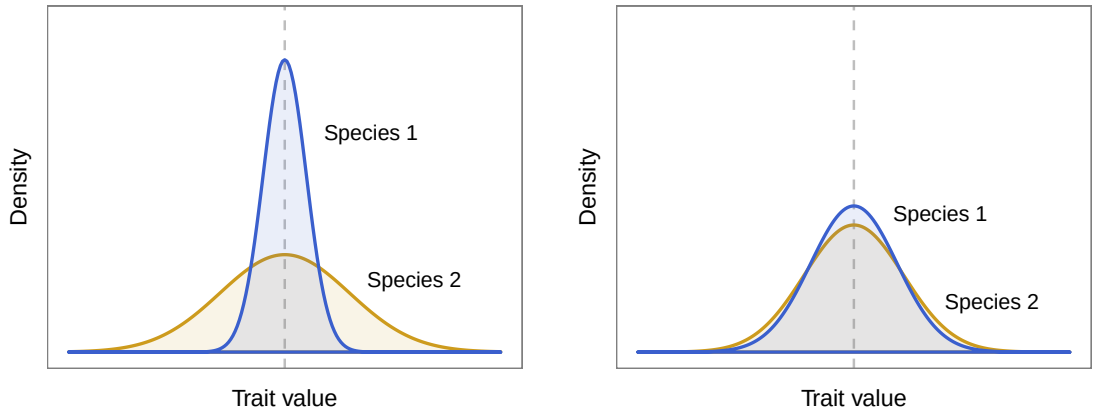

Figure 2: Left: The intensity of interspecific competition between two species with the same mean trait is lowered if their trait variances are different. The reason is that the species with the higher variance has individuals that do not overlap with individuals of the the other species. Right: when two species with the same mean trait have very similar intraspecific variances, the overlap in individuals is not reduced substantially, leading to nonrobust coexistence. The dashed gray line indicates the species' mean trait position.

models only the direction of the vector of intrinsic growth rates matters, but not its magnitude. Indeed, from the equilibrium equations Eq. (3.2), multiplying all b_i values by a positive constant η simply rescales the equilibrium densities by η as well, therefore feasibility is unaffected. Second, the well-known conditions for feasibility in two-species competitive Lotka–Volterra systems read

$$\frac{\alpha_{12}}{\alpha_{22}} < \frac{b_1}{b_2} < \frac{\alpha_{11}}{\alpha_{21}} \tag{3.7}$$

(e.g., Vandermeer 1975, Mallet 2012). These conditions can be written in a slightly different, more geometric form: since only the direction of the intrinsic rates matters, we can parameterize them as $b_1 = \cos\phi$, $b_2 = \sin\phi$. Then the vector (b_1, b_2) has length 1, and $0 < \phi < \pi/2$ is the angle measured counterclockwise from the abscissa of the plane of possible intrinsic growth rate vectors. Substituting this into Eq. (3.7) and simplifying, we get

$$\arctan\left(\frac{\alpha_{21}}{\alpha_{11}}\right) < \phi < \arctan\left(\frac{\alpha_{22}}{\alpha_{12}}\right). \tag{3.8}$$

Using Eq. (3.3), this reads

$$\arctan\left(\mathrm{e}^{-\frac{d^2}{2\sigma_1^2+2\sigma_2^2+\omega^2}}\sqrt{\frac{4\sigma_1^2+\omega^2}{2\sigma_1^2+2\sigma_2^2+\omega^2}}\right) < \phi < \arctan\left(\mathrm{e}^{\frac{d^2}{2\sigma_1^2+2\sigma_2^2+\omega^2}}\sqrt{\frac{2\sigma_1^2+2\sigma_2^2+\omega^2}{4\sigma_2^2+\omega^2}}\right), \tag{3.9}$$

fully characterizing the set of parameters compatible with coexistence as a function of the trait means and variances (Figure 3).

We can also express the fraction of ϕ values leading to feasibility, out of all possible values $0 < \phi < \pi/2$, by rearranging the above inequalities. Calling this fraction Ξ, we get

$$\Xi = \frac{2}{\pi}\left[\arctan\left(\mathrm{e}^{\frac{d^2}{2\sigma_1^2+2\sigma_2^2+\omega^2}}\sqrt{\frac{2\sigma_1^2+2\sigma_2^2+\omega^2}{4\sigma_2^2+\omega^2}}\right) - \arctan\left(\mathrm{e}^{-\frac{d^2}{2\sigma_1^2+2\sigma_2^2+\omega^2}}\sqrt{\frac{4\sigma_1^2+\omega^2}{2\sigma_1^2+2\sigma_2^2+\omega^2}}\right)\right]. \tag{3.10}$$

In the absence of intraspecific variation ($\sigma_1 = \sigma_2 = 0$), this simplifies to

$$\Xi_0 = \frac{2}{\pi}\left[\arctan\left(\mathrm{e}^{d^2/\omega^2}\right) - \arctan\left(\mathrm{e}^{-d^2/\omega^2}\right)\right] \tag{3.11}$$

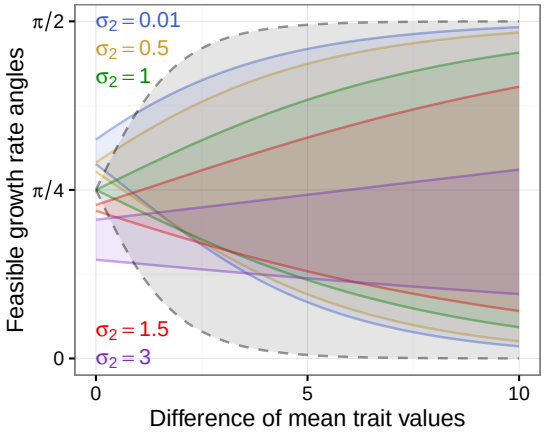

Figure 3: The range of angles of the intrinsic growth rate vector (b_1, b_2) (measured counterclockwise from the abscissa) allowing for two-species coexistence as a function of mean trait distance, for various values of intraspecific variability σ_2 (see legend). Here $\sigma_1 = 1$ and $\omega = 1.1$. Lines denote the lower and upper boundaries of the shaded coexistence region. The black region with dashed boundaries is the reference case with no intraspecific variability: $\sigma_1 = \sigma_2 = 0$. Unless mean trait differences are very small, the case without intraspecific variation always leads to a larger feasibility domain.

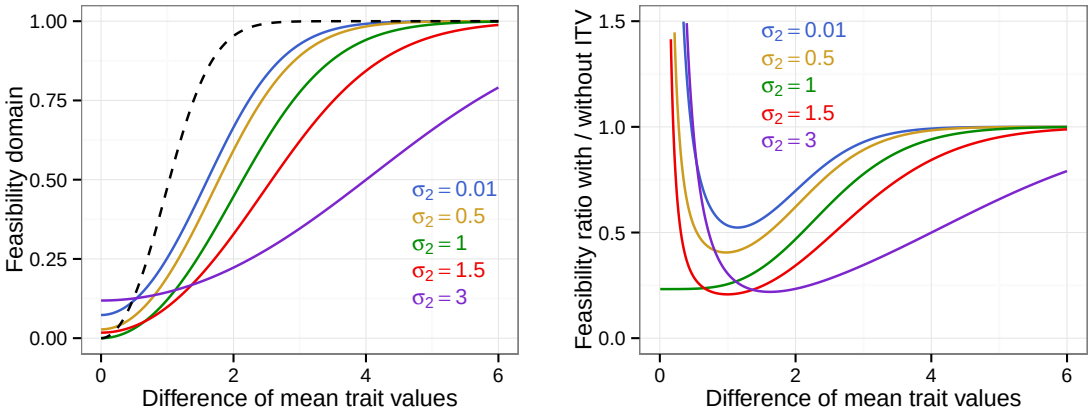

Figure 4: As Figure 1, but plotting the fraction of feasible parameter space Ξ (left) and the ratios Ξ/Ξ_0 (right). The qualitative picture is the same as before, except all feasibility ratios converge to one for d large. This is because as $d \to \infty$, the interspecific interaction coefficients approach zero, and the system decouples into two independent, logistically growing species. Any single species following logistic growth is viable as long as its intrinsic growth rate is positive, regardless of whether there is any intraspecific variability. Therefore, the feasibility ratios with- and without intraspecific variation converge to one as d increases.

The feasibility domains Ξ and Ξ_0 as well as their ratio may be plotted just as the determinants were (Figure 4). The exact same qualitative picture emerges as before. A quantitative difference is that Ξ/Ξ_0 always asymptotes at one for $d \to \infty$, whereas the determinant ratios do not. The reason is that when the two species are sufficiently far apart they decouple into two independent logistic species, with feasibility ensured for any positive intrinsic growth rate, regardless of intraspecific variation. The ratio of the two feasibility domains is therefore equal to one for d large.

3.3 The eco-evolutionary dynamics

For a single species, the eco-evolutionary dynamics given by Eqs. (2.10) and (2.11) is simple. The equilibrium density is the solution to $\mathrm{d}N/\mathrm{d}t = N(b-\alpha N) = 0$, yielding $\hat{N} = b/\alpha = b\sqrt{1+(2\sigma/\omega)^2}$, where Eq. (2.19) was used to express $\alpha = \alpha_{ii}$. This solution is feasible as long as b is positive. The evolutionary dynamics reads $\mathrm{d}\mu/\mathrm{d}t = h^2(\overline{b}-\beta N)$. Unless $h^2 = 0$, the evolutionary equilibrium is given by $\overline{b} = \beta\hat{N}$, but since $\beta = \beta_{ii} = 0$ from Eq. (2.20), we are left with $\overline{b} = 0$. That is, any of the roots of $\overline{b}$ may serve as evolutionary fixed points depending on initial conditions; local stability is ensured by $\overline{b}$ having a negative slope at the corresponding root as a function of the mean trait μ.

For two species, Figures 5 and 6 show different scenarios with stable coexistence. In the first example the two species experience character divergence, while in the second the evolutionarily stable strategy involves both species having equal mean trait values. Of course, whether we see the convergence or divergence of the mean traits also depends on initial conditions (imagine Figure 5 with initial conditions $\mu_1(0) = -5$, $\mu_2(0) = 5$). However, it is of special interest to see when one can expect the perfect convergence of the two species' mean traits.

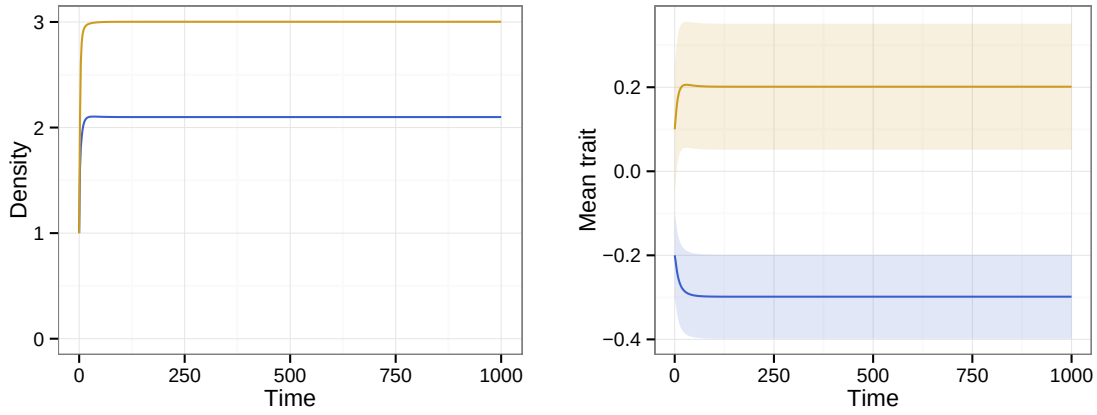

Figure 5: Left panel: population densities of the two species in time. Right panel: the mean trait of the two species in time; the shaded regions mark the $\pm\sigma_i$ regions around the mean. The two species diverge in their mean traits, ending up with coexistence in line with classical limiting similarity. We use the rectangular growth function (Section 2.3) with parameter values $\theta = 0.5$, $\omega = 0.1$, $h_1^2 = h_2^2 = 0.5$, $\sigma_1 = 0.1$, $\sigma_2 = 0.15$, and initial conditions $N_1(0) = 1$, $N_2(0) = 1$, $\mu_1(0) = -0.2$, $\mu_2(0) = 0.1$.

To this end, let us assume that the two species have an evolutionary equilibrium at $\mu_1 = \mu_2 = 0$; this can be achieved by choosing $b(z)$ to be symmetric around $z = 0$. In that case, $\overline{b}_i$ is zero because Eq. (2.7) reduces to the integral of the product of symmetric and antisymmetric functions, and β_{ij} is also zero by Eq. (2.20). Then, from Eq. (2.11), we see that $\mu_1 = \mu_2 = 0$ is indeed an evolutionary equilibrium. We will also assume equal heritabilities ($h_1^2 = h_2^2 = h^2$), and that $b(z)$ is nonnegative. We can write out the Jacobian J for two species, using Eq. (2.14):

$$J = \begin{pmatrix} b_1 - 2\alpha_{11}N_1 - \alpha_{12}N_2 & -\alpha_{12}N_1 & N_1\frac{\partial b_1}{\partial \mu_1} - N_1N_2\frac{\partial \alpha_{12}}{\partial \mu_1} & -N_1N_2\frac{\partial \alpha_{12}}{\partial \mu_2} \\ -\alpha_{21}N_2 & b_2 - \alpha_{21}N_1 - 2\alpha_{22}N_2 & -N_1N_2\frac{\partial \alpha_{21}}{\partial \mu_1} & N_2\frac{\partial b_2}{\partial \mu_2} - N_1N_2\frac{\partial \alpha_{21}}{\partial \mu_2} \\ -h^2\beta_{11} & -h^2\beta_{12} & h^2\left(\frac{\partial \overline{b}_1}{\partial \mu_1} - 2N_1\frac{\partial \beta_{11}}{\partial \mu_1} - N_2\frac{\partial \beta_{12}}{\partial \mu_1}\right) & -h^2N_2\frac{\partial \beta_{12}}{\partial \mu_2} \\ -h^2\beta_{21} & -h^2\beta_{22} & -h^2N_1\frac{\partial \beta_{21}}{\partial \mu_1} & h^2\left(\frac{\partial \overline{b}_2}{\partial \mu_2} - N_1\frac{\partial \beta_{21}}{\partial \mu_2} - 2N_2\frac{\partial \beta_{22}}{\partial \mu_2}\right) \end{pmatrix}. \tag{3.12}$$

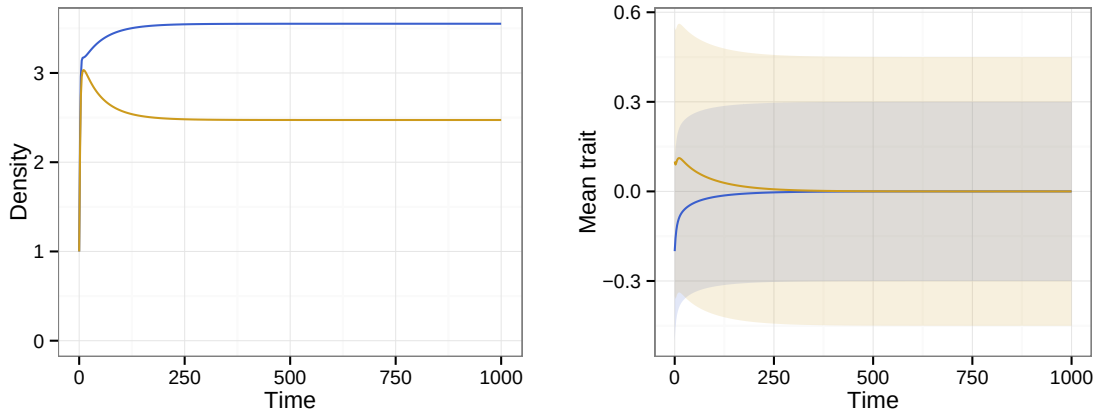

Figure 6: As Figure 5, except with $\sigma_1 = 0.3$ and $\sigma_2 = 0.45$ (they are both three times what they were before). The mean traits now converge to be equal, but because the intraspecific variances are different, the blue species is a specialist and the yellow is a generalist. The example demonstrates that the evolutionary outcome can be changed from character divergence to convergence simply by rescaling the intraspecific standard deviations.

At the (stable or unstable) evolutionary equilibrium $\mu_1 = \mu_2 = 0$, further simplifications are available: $\beta_{11} = \beta_{22} = 0$, and $\partial\alpha_{ij}/\partial\mu_k = 0$ for all $i, j, k = 1, 2$. Also, since $b(z)$ is symmetric, it has an extremum around $z = 0$. Then, by Eq. (2.3), so does b_i around $\mu_i = 0$:

$$\frac{\partial b_i}{\partial \mu_i} = \frac{\partial}{\partial \mu_i} \int p_i(z) b(z)\, \mathrm{d}z = \int \frac{\partial p_i(z)}{\partial \mu_i} b(z)\, \mathrm{d}z, \tag{3.13}$$

which, for $\mu_i = 0$, is the integral of the product of an antisymmetric and a symmetric function, evaluating to zero. Therefore, $\partial b_i/\partial \mu_j = 0$ for all $i, j = 1, 2$. We then have

$$J = \begin{pmatrix} b_1 - 2\alpha_{11}N_1 - \alpha_{12}N_2 & -\alpha_{12}N_1 & 0 & 0 \\ -\alpha_{21}N_2 & b_2 - \alpha_{21}N_1 - 2\alpha_{22}N_2 & 0 & 0 \\ 0 & 0 & h^2\left(\frac{\partial \bar{b}_1}{\partial \mu_1} - 2N_1 \frac{\partial \beta_{11}}{\partial \mu_1} - N_2 \frac{\partial \beta_{12}}{\partial \mu_1}\right) & -h^2 N_2 \frac{\partial \beta_{12}}{\partial \mu_2} \\ 0 & 0 & -h^2 N_1 \frac{\partial \beta_{21}}{\partial \mu_1} & h^2\left(\frac{\partial \bar{b}_2}{\partial \mu_2} - N_1 \frac{\partial \beta_{21}}{\partial \mu_2} - 2N_2 \frac{\partial \beta_{22}}{\partial \mu_2}\right) \end{pmatrix}, \tag{3.14}$$

which is the direct sum of two independent 2×2 blocks—the top block corresponds to the dynamics of the densities, the bottom one to the trait means. Therefore, in this case the dynamics of the local abundances and trait means are decoupled, making the analysis much simpler. As we have shown in Section 3.1, the top 2×2 block of the Jacobian is necessarily stable when $-\alpha_{ij}$ is symmetric and all its entries are negative; this block describes meaningful coexistence when the feasibility condition Eq. (3.7) is also satisfied.

Local stability of the bottom 2×2 block of Eq. (3.14) would mean that the two species experience convergent evolution, at least in the vicinity of $\mu_1 = \mu_2 = 0$. Using Eq. (3.2) for the equilibrium densities, one can calculate the two eigenvalues to determine whether the $\mu_1 = \mu_2 = 0$ evolutionary equilibrium is stable; both eigenvalues having negative real parts means stability. Equivalently, one may use the Routh–Hurwitz criteria (Edelstein-Keshet 1988): any 2×2 matrix is stable if and only if its trace is negative while its determinant is positive.

We introduce some simplifying notation. Let the bottom 2×2 block of J be $J^{(\mu)}$. Also, for any quantity x, let $\tilde{x} = x/\omega$, i.e., we measure quantities in units of ω whenever appropriate, thus eliminating one of the

variables. Let $\overline{b}_i' = \partial \overline{b}_i / \partial \mu_i$ evaluated at $\mu_i = 0$, and let

$$s_i = \sqrt{1 + 4\tilde{\sigma}_i^2}, \tag{3.15}$$

$$s_{ij} = \sqrt{1 + 2\tilde{\sigma}_i^2 + 2\tilde{\sigma}_j^2}. \tag{3.16}$$

Writing α_{ij} and β_{ij} using Eqs. (2.19) and (2.20) at $\mu_1 = \mu_2 = 0$, we can evaluate $J^{(\mu)}$ at the equilibrium densities $\hat{N}_1$ and $\hat{N}_2$:

$$J^{(\mu)} = h^2 \begin{pmatrix} \overline{b}_1' + 2\hat{N}_2\tilde{\sigma}_1^2/s_{12}^3 & -2\hat{N}_2\tilde{\sigma}_1^2/s_{12}^3 \\ -2\hat{N}_1\tilde{\sigma}_2^2/s_{12}^3 & \overline{b}_2' + 2\hat{N}_1\tilde{\sigma}_2^2/s_{12}^3 \end{pmatrix}. \tag{3.17}$$

The first Routh–Hurwitz criterion is that the trace of this matrix should be negative:

$$\mathrm{tr}(J^{(\mu)}) = h^2 \left(\overline{b}_1' + \overline{b}_2' + 2\frac{\hat{N}_2\tilde{\sigma}_1^2 + \hat{N}_1\tilde{\sigma}_2^2}{s_{12}^3} \right) < 0. \tag{3.18}$$

Rearranging, we get

$$\frac{\hat{N}_2\tilde{\sigma}_1^2 + \hat{N}_1\tilde{\sigma}_2^2}{s_{12}^3} + \frac{\overline{b}_1' + \overline{b}_2'}{2} < 0. \tag{3.19}$$

Similarly, the second Routh–Hurwitz criterion is that the determinant should be positive:

$$\det(J^{(\mu)}) = h^4 \left(\left(\overline{b}_1' + 2\hat{N}_2\tilde{\sigma}_1^2/s_{12}^3 \right) \left(\overline{b}_2' + 2\hat{N}_1\tilde{\sigma}_2^2/s_{12}^3 \right) - \frac{4\hat{N}_1\hat{N}_2\tilde{\sigma}_1^2\tilde{\sigma}_2^2}{s_{12}^6} \right) > 0, \tag{3.20}$$

or

$$\frac{\overline{b}_1'\overline{b}_2'}{2} + \frac{\tilde{\sigma}_1^2\hat{N}_2\overline{b}_2' + \tilde{\sigma}_2^2\hat{N}_1\overline{b}_1'}{s_{12}^3} > 0. \tag{3.21}$$

Note that $\overline{b}_i'$ is necessarily negative: $\overline{b}_i' = -|\overline{b}_i'|$. Indeed, using the definition in Eq. (2.7),

$$\frac{\partial \overline{b}_i}{\partial \mu_i} = \frac{\partial}{\partial \mu_i} \int (z - \mu_i) p_i(z) b(z)\, \mathrm{d}z = \int \left[\frac{\partial (z - \mu_i)}{\partial \mu_i} p_i(z) b(z) + (z - \mu_i) \frac{\partial p_i(z)}{\partial \mu_i} b(z) \right] \mathrm{d}z, \tag{3.22}$$

which, using Eq. (1.5) and evaluating at $\mu_i = 0$, reads

$$\overline{b}_i' = \left. \frac{\partial \overline{b}_i}{\partial \mu_i} \right|_{\mu_i = 0} = -\int p_i(z) b(z)\, \mathrm{d}z - \frac{1}{\sigma_i^2} \int z^2 p_i(z) b(z)\, \mathrm{d}z. \tag{3.23}$$

Both integrals are over products of positive functions; with the negative sign, the expression as a whole is negative. This shows that $\overline{b}_i'$ is necessarily negative.

The equilibrium densities $\hat{N}_1$ and $\hat{N}_2$ can be calculated from Eq. (3.2). The α_{ij} are given by Eq. (3.3) with $d = |\mu_1 - \mu_2| = 0$ which, using Eqs. (3.15) and (3.16), can be written

$$\alpha_{ij} = \begin{pmatrix} 1/s_1 & 1/s_{12} \\ 1/s_{12} & 1/s_2 \end{pmatrix}. \tag{3.24}$$

Inverting this matrix, we get

$$\left(\alpha^{-1}\right)_{ij} = \frac{s_1 s_2 s_{12}^2}{s_{12}^2 - s_1 s_2} \begin{pmatrix} 1/s_2 & -1/s_{12} \\ -1/s_{12} & 1/s_1 \end{pmatrix}. \tag{3.25}$$

Substituting this inverse into Eq. (3.2), we can express the two equilibrium densities:

$$\hat{N}_1 = \frac{s_1 s_{12}(b_1 s_{12} - b_2 s_2)}{s_{12}^2 - s_1 s_2}, \tag{3.26}$$

$$\hat{N}_2 = \frac{s_2 s_{12}(b_2 s_{12} - b_1 s_1)}{s_{12}^2 - s_1 s_2}. \tag{3.27}$$

Substituting these into the Routh–Hurwitz criteria in Eqs. (3.19) and (3.21), we get

$$\frac{|\overline{b}_1'| + |\overline{b}_2'|}{2} > \frac{\tilde{\sigma}_1^2 s_2(b_2 s_{12} - b_1 s_1) + \tilde{\sigma}_2^2 s_1(b_1 s_{12} - b_2 s_2)}{s_{12}^2(s_{12}^2 - s_1 s_2)}, \tag{3.28}$$

$$\frac{|\overline{b}_1'||\overline{b}_2'|}{2} > \frac{\tilde{\sigma}_1^2 s_2(b_2 s_{12} - b_1 s_1)|\overline{b}_2'| + \tilde{\sigma}_2^2 s_1(b_1 s_{12} - b_2 s_2)|\overline{b}_1'|}{s_{12}^2(s_{12}^2 - s_1 s_2)}. \tag{3.29}$$

Eq. (3.28) has the biological interpretation that the average slope of the $\overline{b}_i$ near $\mu = 0$ has to be sufficiently large in magnitude for character convergence to happen. However, the slopes cannot be large when the intraspecific standard deviations are either too small or too large. This is easily verified: for $\sigma_i \to \infty$ the integral in Eq. (2.7) converges to zero for all μ_i because the density of an infinitely wide Gaussian $p_i(z)$ is vanishing at all points (and so the integral's derivative with respect to μ_i is also zero), while for $\sigma_i \to 0$ the trait distribution $p_i(z)$ converges to the Dirac delta distribution $\delta(z - \mu_i)$ and so, using Eq. (2.7),

$$\overline{b}_i' = \frac{\partial}{\partial \mu_i} \int (z - \mu_i)\delta(z - \mu_i) b(z)\, \mathrm{d}z \bigg|_{\mu_i = 0} = \frac{\partial}{\partial \mu_i}(0 \times b(\mu_i)) = 0. \tag{3.30}$$

Then, due to continuity in σ_i, very small or very large phenotypic standard deviations imply small values of $|\overline{b}_i'|$. Its maximum is therefore obtained somewhere in between, when $\tilde{\sigma}_i \approx \tilde{\theta}$. Biologically, this means that the intraspecific standard deviations can be neither simultaneously too small nor simultaneously too large compared with the width of $b(z)$, otherwise we do not observe the convergence of the mean traits. Using Eqs. (3.28) and (3.29), Figure 7 shows the precise parameter region where one obtains convergent evolution, for the case of the rectangular growth function (Section 2.3).

Of course, evolutionary convergence does not guarantee that both species can maintain positive densities at the evolutionary equilibrium $\mu_1 = \mu_2 = 0$. For that, the ecological equilibrium must be locally stable and feasible. As discussed before, the top 2×2 block of J is necessarily stable, therefore the only question is that of feasibility. The two-species feasibility condition is given by Eq. (3.7); for the rectangular growth function (Section 2.3), this reads

$$\frac{1 + 4\tilde{\sigma}_2^2}{1 + 2\tilde{\sigma}_1^2 + 2\tilde{\sigma}_2^2} < \frac{\mathrm{erf}^2\left(\tilde{\theta}/(\sqrt{2}\tilde{\sigma}_1)\right)}{\mathrm{erf}^2\left(\tilde{\theta}/(\sqrt{2}\tilde{\sigma}_2)\right)} < \frac{1 + 2\tilde{\sigma}_1^2 + 2\tilde{\sigma}_2^2}{1 + 4\tilde{\sigma}_1^2}. \tag{3.31}$$

In particular, these inequalities are very difficult to satisfy when $\tilde{\sigma}_1 \approx \tilde{\sigma}_2$, and become impossible to do so for $\tilde{\sigma}_1 = \tilde{\sigma}_2$. In order to observe trait convergence which also ends up in ecological coexistence, one therefore needs sufficient segregation of the species in their intraspecific standard deviations. Roughly speaking, one species must be a generalist and the other a specialist consumer.

The robust possibility of convergent trait evolution points to the fact that measuring species similarity purely on the basis of trait means can be misleading. Coexistence can result from segregation along the trait axis (Figure 5), but also from having similar mean traits but different intraspecific standard deviations (Figure 6). Limiting similarity in the classical sense (MacArthur and Levins 1967) therefore has to be extended in the presence of intraspecific trait variation: its naive application to the trait means without taking the variances into account may lead to the incorrect conclusion that two species coexist without niche segregation, when they are in fact niche-segregated.

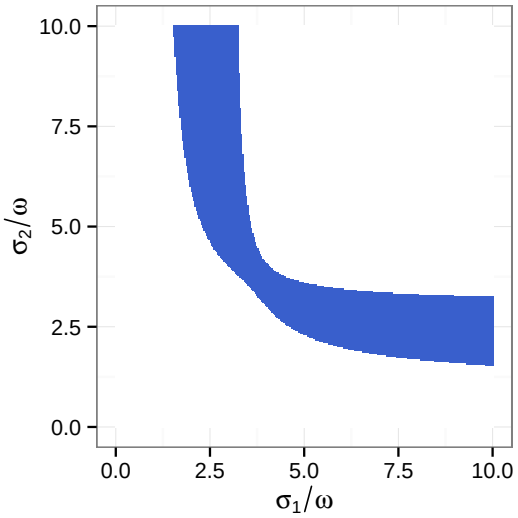

Figure 7: Region of convergent evolution (blue strip) as a function of the scaled intraspecific standard deviations $\tilde{\sigma}_1$ and $\tilde{\sigma}_2$. The growth function is rectangular (Section 2.3); the value of $\tilde{\theta}$ is set to 5. The blue region shows where the Routh–Hurwitz criteria of Eqs. (3.28) and (3.29) are satisfied; i.e., in this region the species evolve identical mean traits. In general, if one standard deviation is high, then the other must be intermediate to get the evolution of the mean traits, resulting in a generalist and a specialist species.

3.4 Robustness of the two-species results to an asymmetry in intrinsic growth

How sensitive are our results to breaking the perfect symmetry of the intrinsic growth function $b(z)$? To examine this, let us introduce an asymmetry in $b(z)$ to see if we can still get character convergence. The difficulty with doing this lies in the fact that, after perturbing $b(z)$, one has to recalculate $b_i(t)$ and $\overline{b}_i(t)$ via Eqs. (2.3) and (2.7). Unfortunately, these integrals cannot in general be evaluated in explicit form, except in certain very simple cases.

The idea for introducing asymmetry in a tractable way is to assume that it is small, so one can expand it to linear order. Instead of the original $b_i(t)$ given by Eq. (2.3), we use the perturbed

$$b_i^*(t) = \int b(z)(1+\eta(z))p_i(z,t)\,\mathrm{d}z. \tag{3.32}$$

If the perturbing function $\eta(z)$ is small and has a nonvanishing first moment, then we can Taylor expand it as $\eta(z) \approx cz$, where c is a constant (we choose η such that the 0th-order term in the expansion is zero). We then can write

$$\begin{aligned} b_i^*(t) &\approx \int b(z)(1+cz)p_i(z,t)\,\mathrm{d}z = b_i(t) + c\int zb(z)p_i(z,t)\,\mathrm{d}z \\ &= b_i(t) + c\int (z-\mu_i(t))b(z)p_i(z,t)\,\mathrm{d}z + c\mu_i(t)\int b(z)p_i(z,t)\,\mathrm{d}z \\ &= (1+c\mu_i(t))b_i(t) + c\overline{b}_i(t). \end{aligned} \tag{3.33}$$

Similarly, instead of $\overline{b}_i(t)$ given by Eq. (2.7), we have

$$\begin{aligned} \overline{b}_i^*(t) &\approx \int (z-\mu_i(t))b(z)(1+cz)p_i(z,t)\,\mathrm{d}z = \overline{b}_i(t) + c\int z(z-\mu_i(t))b(z)p_i(z,t)\,\mathrm{d}z \\ &= \overline{b}_i(t) + c\int \Big[(z-\mu_i(t))^2 + \mu_i(t)(z-\mu_i(t))\Big]b(z)p_i(z,t)\,\mathrm{d}z. \end{aligned} \tag{3.34}$$

Defining $\hat{b}_i(t)$ as

$$\hat{b}_i(t) = \int (z-\mu_i(t))^2 b(z) p_i(z,t)\,\mathrm{d}z \tag{3.35}$$

(i.e., the second central moment), we can continue writing

$$\begin{aligned}\overline{b}_i^*(t) &\approx \overline{b}_i(t) + c\int \Big[(z-\mu_i(t))^2 + \mu_i(t)(z-\mu_i(t))\Big] b(z)p_i(z,t)\,\mathrm{d}z \\ &= \overline{b}_i(t) + c\int (z-\mu_i(t))^2 b(z)p_i(z,t)\,\mathrm{d}z + c\mu_i(t)\int (z-\mu_i(t))b(z)p_i(z,t)\,\mathrm{d}z \\ &= (1+c\mu_i(t))\overline{b}_i(t) + c\hat{b}_i(t).\end{aligned} \tag{3.36}$$

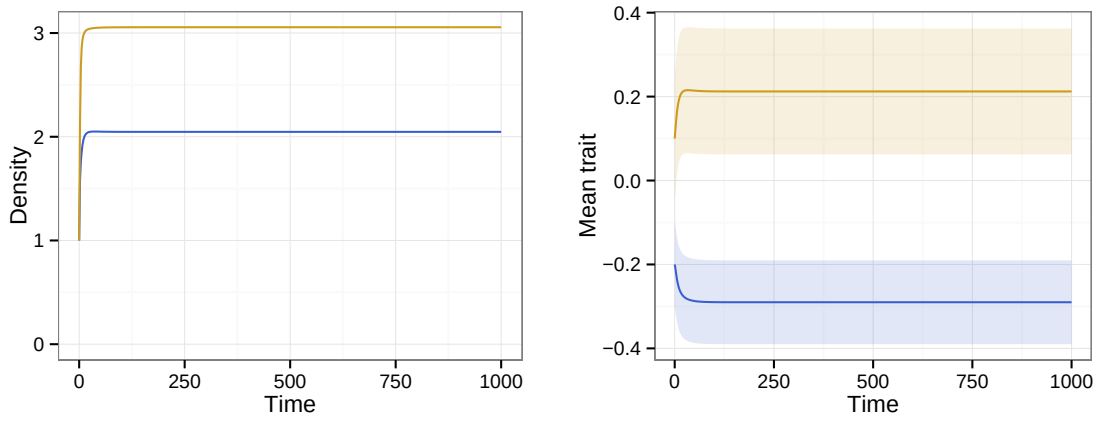

Figure 8: As Figure 5, except with an asymmetry in the intrinsic growth function $b(z)(1+cz)$, with $c = 0.1$.

The advantage of this approach is highlighted by the fact that $\hat{b}_i(t)$ can be explicitly integrated, depending on parameterization (Section 2.3):

I. $b(z)$ rectangular:

$$\begin{aligned}\hat{b}_i(t) = \frac{\sigma_i^2}{2}&\left[\mathrm{erf}\left(\frac{\theta-\mu_i(t)}{\sqrt{2}\sigma_i}\right) + \mathrm{erf}\left(\frac{\theta+\mu_i(t)}{\sqrt{2}\sigma_i}\right)\right] \\ &+ \frac{1}{\sqrt{2\pi}}\exp\left(-\frac{(\theta+\mu_i(t))^2}{2\sigma_i^2}\right)\left[(\mu_i(t)-\theta)\sigma_i \exp\left(\frac{2\theta\mu_i(t)}{\sigma_i^2}\right) - (\mu_i(t)+\theta)\sigma_i\right].\end{aligned} \tag{3.37}$$

II. $b(z)$ quadratic:

$$\begin{aligned}\hat{b}_i(t) = \frac{\sigma_i^2}{2\theta^2}&\left\{(\theta^2-\mu_i^2(t)-3\sigma_i^2)\left[\mathrm{erf}\left(\frac{\theta-\mu_i(t)}{\sqrt{2}\sigma_i}\right) + \mathrm{erf}\left(\frac{\theta+\mu_i(t)}{\sqrt{2}\sigma_i}\right)\right]\right. \\ &\left.+ \sqrt{\frac{2}{\pi}}\sigma_i \exp\left(-\frac{(\theta+\mu_i(t))^2}{2\sigma_i^2}\right)\left[(3\theta+\mu_i(t))\exp\left(\frac{2\theta\mu_i(t)}{\sigma_i^2}\right) + 3\theta - \mu_i(t)\right]\right\}.\end{aligned} \tag{3.38}$$

III. $b(z)$ triangular:

$$\begin{aligned}\hat{b}_i(t) = \frac{\sigma_i^2}{4\theta}&(\theta+\mu_i(t))\left[\mathrm{erf}\left(\frac{\theta-\mu_i(t)}{\sqrt{2}\sigma_i}\right) + \mathrm{erf}\left(\frac{\theta+\mu_i(t)}{\sqrt{2}\sigma_i}\right)\right] \\ &+ \frac{\sigma_i}{\sqrt{2\pi}\theta}\exp\left(-\frac{(\theta+\mu_i(t))^2}{2\sigma_i^2}\right)\left[\sigma_i^2 - \exp\left(\frac{2\theta\mu_i(t)}{\sigma_i^2}\right)(\theta^2+\sigma_i^2-\theta\mu_i(t))\right].\end{aligned} \tag{3.39}$$

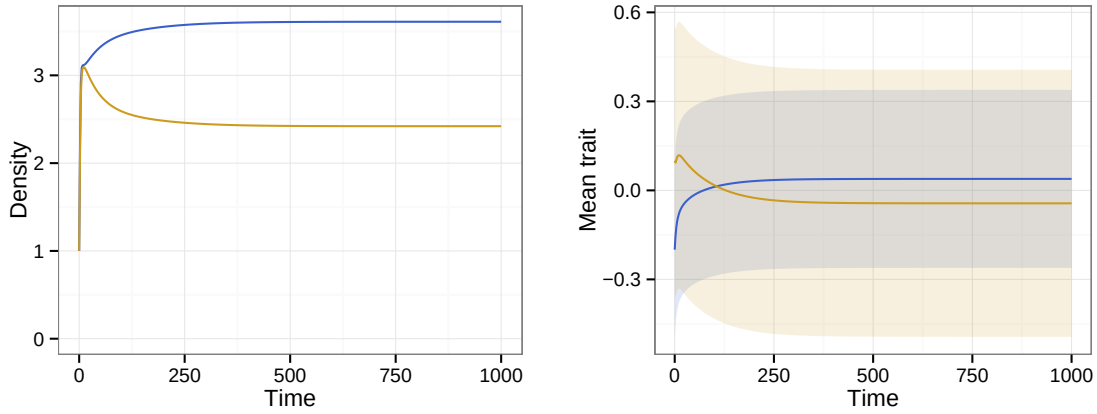

Figure 9: As Figure 6, except with an asymmetry in the intrinsic growth function $b(z)(1+cz)$, with $c = 0.1$.

When the intraspecific standard deviations are low, then predictably, asymmetry does not alter qualitative behavior, and we get the same result as before (Figure 8, which is much the same as Figure 5 despite the added asymmetry). However, on Figure 9, which is set up just like Figure 6 plus the asymmetry, the two species no longer evolve the exact same mean trait. In and of itself, this is not very surprising, because for $b(z)$ asymmetric, $\mu_1 = \mu_2 = 0$ can no longer in general be expected to be a fixed point of the evolutionary dynamics. However, the difference $d = |\mu_1 - \mu_2|$ in mean traits is slight, especially compared with the two intraspecific standard deviations. This holds even though the amount of introduced asymmetry is in fact not very small (Figure 10).

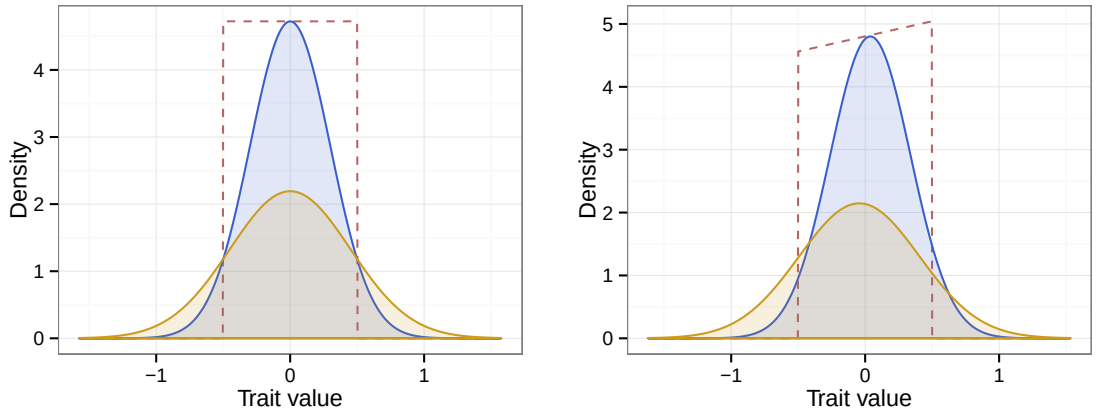

Figure 10: Equilibrium state of two-species communities, with- and without asymmetry in intrinsic growth (left and right panels, respectively). Both panels used the rectangular growth function (Section 2.3), and parameter values $\theta = 5$, $\omega = 1$, $h_1^2 = h_2^2 = 0.5$, $\sigma_1 = 3$, $\sigma_2 = 4.5$, starting from initial conditions $N_1(0) = 1$, $N_2(0) = 1$, $\mu_1(0) = -2$, $\mu_2(0) = 1$. The asymmetry parameter is set to $c = 0$ (left panel) and $c = 0.1$ (right panel). The shaded regions are the density distributions of the two species at equilibrium as a function of trait value. The dashed red line in each panel (not drawn to scale) is the intrinsic growth function $b(z)(1+cz)$, where $b(z)$ is given by Eq. (2.21). On the left, the two species evolve the same mean trait, but on the right their alignment is not perfect due to the asymmetry.

In summary, though the species no longer evolve the exact same mean trait as a stable evolutionary outcome in the presence of asymmetry, it is nevertheless still true that, for sufficiently large intraspecific

standard deviations, the difference in their mean traits will be small compared to their σs, and so it is still true that the two species represent a specialist and a generalist type.

4 Multispecies results

4.1 Multiple species with equal intraspecific variances and no heritability

Here we study a simple reference case for which an exact answer can be given to the question of how intraspecific variability affects expected species richness. To this end, we make two assumptions. First, all heritabilities are zero: intraspecific variation is purely plastic. Second, each species has the same intraspecific standard deviation σ.

The competition coefficients α_{ij} are given by Eq. (2.19), which reduces to

$$\alpha_{ij} = \frac{\omega}{\sqrt{4\sigma^2+\omega^2}} \exp\left(-\frac{(\mu_i-\mu_j)^2}{4\sigma^2+\omega^2}\right) \tag{4.1}$$

when all the σs are equal. In the absence of intraspecific variation, the competition coefficients are instead given by Eq. (2.18):

$$\alpha_{ij} = \exp\left(-\frac{(\mu_i-\mu_j)^2}{\omega^2}\right), \tag{4.2}$$

which can also be obtained by taking the $\sigma \to 0$ limit in Eq. (4.1). If the heritabilities are zero, then species do not evolve, and the only difference between the model with- and without intraspecific variation is that the competition coefficients have a different form, given by Eqs. (4.1) and (4.2).

The number of coexisting species in a Lotka–Volterra trait axis model *without* intraspecific trait variation is proportional to the inverse of the competition width ω in Eq. (4.2) (MacArthur and Levins 1967, Szabó and Meszéna 2006, Scheffer and van Nes 2006, Barabás and Meszéna 2009), a rule of thumb that holds unless parameters are carefully (and unbiologically) fine-tuned (Barabás et al. 2012). However, when all σs are equal, one can think of the model *with* intraspecific variation as an effective model for a community *without* such variation, but with the modified competition coefficients given by Eq. (4.1). The competition width of these effective coefficients is $\sqrt{4\sigma^2+\omega^2}$. The ratio of predicted species richnesses with- and without intraspecific variation is therefore $\omega/\sqrt{4\sigma^2+\omega^2}$. Equivalently, we can also write $1/\sqrt{4\tilde{\sigma}^2+1}$ for the ratio, where $\tilde{\sigma} = \sigma/\omega$. Figure 11 compares this analytical prediction with simulation results, starting from the same initial conditions and varying σ for two different values of ω.

The important conclusions about species richness are as follows. First, intraspecific variability has an overall negative effect on species diversity. Second, this negative effect increases monotonically with σ. Third, for very small amounts of intraspecific variability, there is practically no effect, since $1/\sqrt{4\tilde{\sigma}^2+1} \approx 1$ for $\tilde{\sigma}$ small. Fourth, for large $\tilde{\sigma}$, $1/\sqrt{4\tilde{\sigma}^2+1} \approx (2\tilde{\sigma})^{-1}$, therefore the decline in species richness will be roughly inversely proportional to $2\sigma/\omega$.

4.2 Measuring community robustness

Local stability of an ecological community in the final state is guaranteed if the community matrix $M_{ij} = -\hat{N}_i\alpha_{ij}$ given in Eq. (2.17) has all its eigenvalues lying in the left half of the complex plane. Here $\hat{N}_i$ is the equilibrium density of species i, and the α_{ij} are given by Eq. (2.19). The real part of an eigenvalue measures the rate of decay (or amplification, if the real part is positive) of a dynamical perturbation along the corresponding eigendirection; small negative real parts indicate slow return times.

The eigenvalues of the community matrix are also related to the robustness of the community. A robust system is one that does not change its qualitative behavior in response to parameter perturbations. Intuitively,

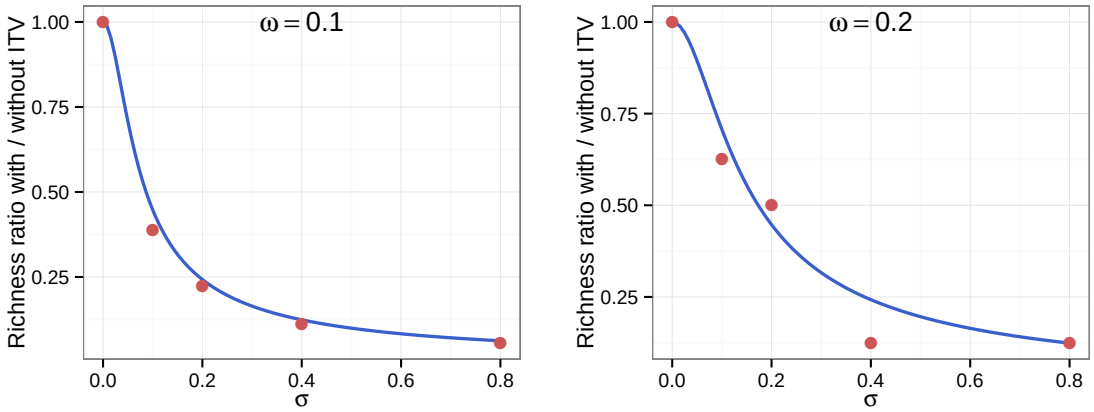

Figure 11: Comparison of the analytically predicted ratio of species richnesses with- and without intraspecific variation, $\omega/\sqrt{4\sigma^2+\omega^2}$ (blue curves) to simulated ones (red dots; obtained with the rectangular $b(z)$ of Section 2.3). Left panel: $\omega = 0.1$; right panel: $\omega = 0.2$. There is more scatter on the right because the average number of species with $\omega = 0.2$ is half the number with $\omega = 0.1$. Since the number of coexisting species must be an integer, rounding errors are expected to be larger when the number of species is small to begin with.

the reason the eigenvalues measure robustness is that their position in the complex plane is a continuous function of model parameters. If an eigenvalue is close to the imaginary axis, then even a small parameter perturbation may push it over to the right half plane, destabilizing the system. More precisely, the magnitude of the community matrix's determinant is a measure of the local robustness of a deterministic dynamical system (Levins 1968, May 1973, Levins 1974, Bender et al. 1984, Yodzis 1988, 2000, Dambacher et al. 2002, Meszéna et al. 2006, Novak et al. 2011, Yeakel et al. 2011, Barabás et al. 2012, Aufderheide et al. 2013, Barabás et al. 2014a,b). The intuition about the eigenvalues measuring robustness is then justified by recognizing that the determinant is the product of all eigenvalues. The Sth root of its absolute value is therefore the (geometric) mean of the eigenvalues' moduli: denoting the ith eigenvalue of M by λ_i, we have

$$\begin{aligned}\sqrt[S]{|\det(M)|} = \sqrt[S]{|\lambda_1 \cdot \ldots \cdot \lambda_S|} = \sqrt[S]{|\lambda_1| \cdot \ldots \cdot |\lambda_S|} = \left(\prod_{i=1}^{S} |\lambda_i|\right)^{1/S} \\ = \exp\left(\frac{1}{S}\log\left(\prod_{i=1}^{S}|\lambda_i|\right)\right) = \exp\left(\frac{1}{S}\sum_{i=1}^{S}\log(|\lambda_i|)\right) = \exp\left(\overline{\log(|\lambda|)}\right),\end{aligned} \tag{4.3}$$

where the overbar denotes (arithmetic) averaging. This quantity can be interpreted as the geometric mean of the return times along each eigendirection, which is especially useful for comparing the robustness of systems with different numbers of species (Barabás et al. 2014b). The determinant itself cannot be used for such comparisons, because its units are $[\text{time}]^{-S}$, which will be different for communities with different numbers of species. In contrast, the units of the geometric mean are always $[\text{time}]^{-1}$, comparable across systems. We call this quantity the "average community robustness".

There is another aspect to robustness. Imagine a two-species community whose community matrix has eigenvalues $\lambda_1 = \lambda_2 = -1$. The geometric mean of their magnitudes is 1. Now take another two-species system with eigenvalues $\lambda_1 = -100$ and $\lambda_2 = -0.01$. The geometric mean is still equal to 1, but the situation is now very different. In the first example, the dynamics are equally robust along both eigendirections. In the second, the first eigendirection is very robust, but the second one is not robust at all. This indicates that this second system will be completely insensitive to some types of parameter perturbations, but extremely

sensitive to others. It is therefore also of interest to see not just how robust a system is to the average environmental disturbance, but whether it reacts strongly to specific disturbances. This can be measured by the geometric standard deviation of the eigenvalues' magnitudes:

$$\exp\left(\sqrt{\overline{\log^2(|\lambda|)} - \overline{\log(|\lambda|)}^2}\right) = \exp\left(\sqrt{\frac{1}{S}\sum_{i=1}^{S}\log^2(|\lambda_i|) - \left(\frac{1}{S}\sum_{i=1}^{S}\log(|\lambda_i|)\right)^2}\right). \tag{4.4}$$

We dub this quantity "robustness heterogeneity", i.e., the degree to which the system's eigendirections vary in their individual robustness.

4.3 The effect of intraspecific variation and heritability on species richness, trait pattern, and community robustness

Here we show all our results generated using the rectangular $b(z)$ given in Eq. (2.21), and the triangular $b(z)$ given in Eq. (2.27). The plots are analogous to Figures 4, 5, and 6 in the main text (where the quadratic $b(z)$, given by Eq. (2.24), was used). The quantitative details are different, but the qualitative results are unaffected by the choice of $b(z)$.

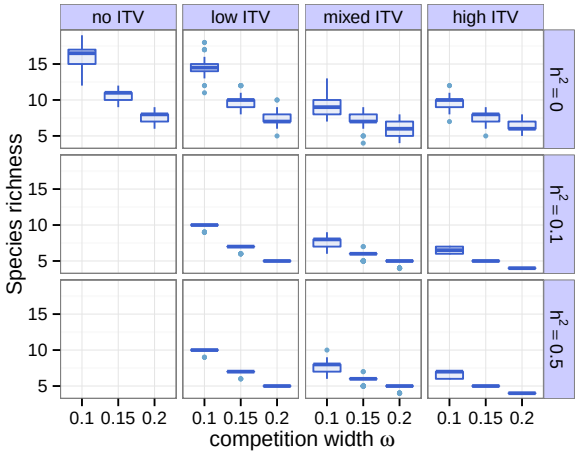

Figure 12: As Figure 4 in the main text, except showing results with $b(z)$ rectangular (Eq. 2.21).

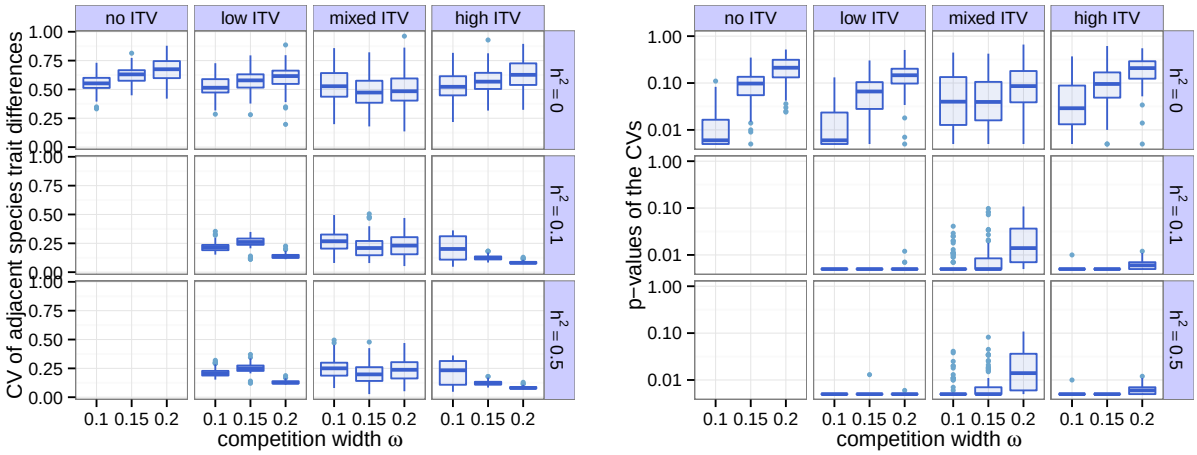

Figure 13: As Figure 5 in the main text, except showing results with $b(z)$ rectangular (Eq. 2.21).

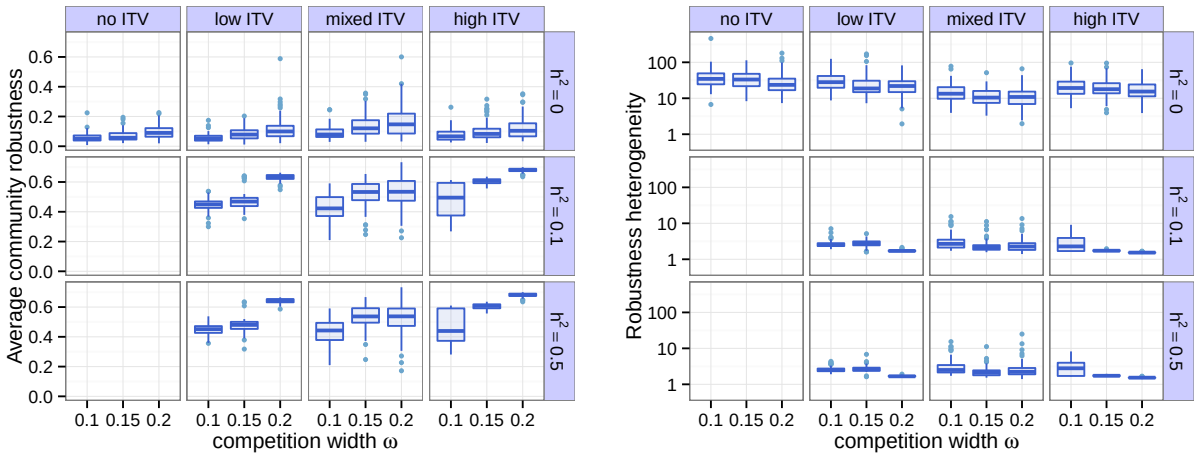

Figure 14: As Figure 6 in the main text, except showing results with $b(z)$ rectangular (Eq. 2.21).

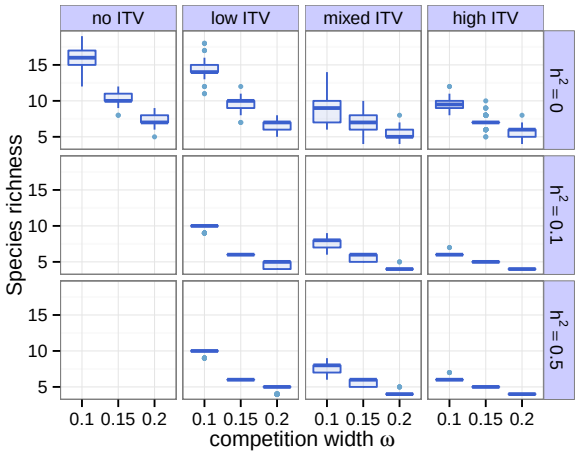

Figure 15: As Figure 4 in the main text, except showing results with $b(z)$ triangular (Eq. 2.27).

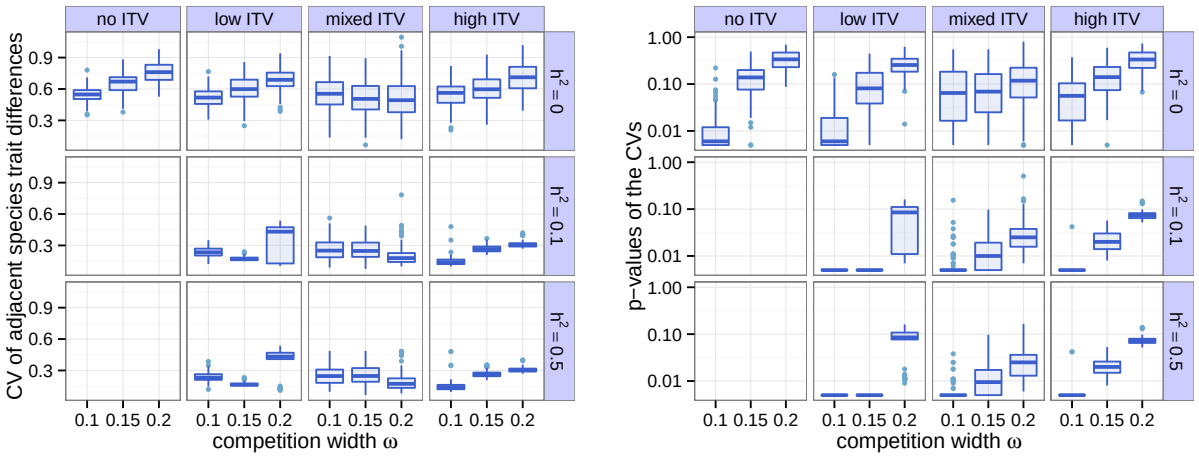

Figure 16: As Figure 5 in the main text, except showing results with $b(z)$ triangular (Eq. 2.27).

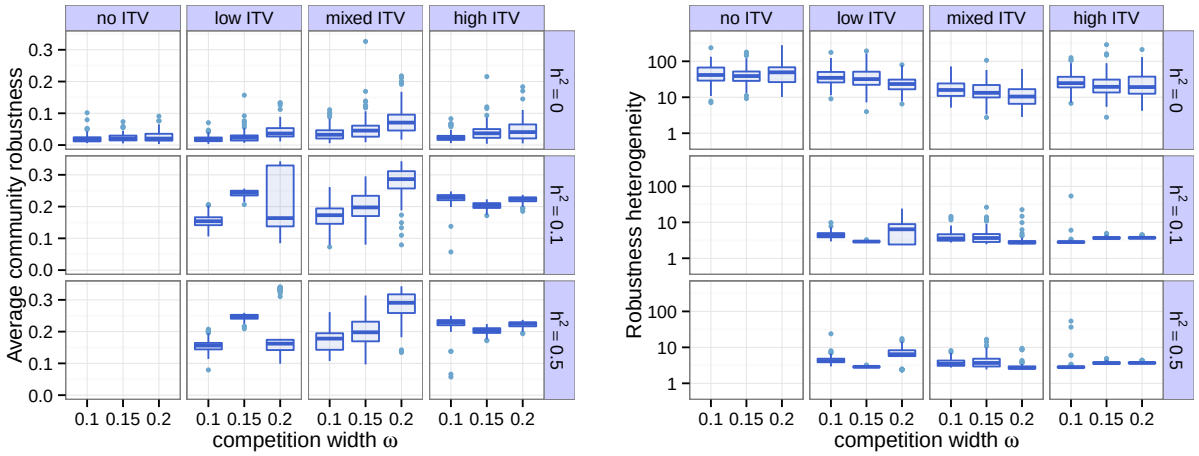

Figure 17: As Figure 6 in the main text, except showing results with $b(z)$ triangular (Eq. 2.27).

4.4 Trait convergence in multispecies communities

In Section 3.3, the possibility of the evolutionary convergence of the trait means of two species was discussed. One important question is whether we observe such convergent evolution in our multispecies simulated communities. The answer is: yes, but only sporadically. Assuming $h^2 > 0$, we counted the total number of simulations where the minimum trait difference between two coexisting species was less than 0.03: it was 60 cases altogether (a little over one percent of all cases with $h^2 > 0$). We can do the same for simulations where the minimum difference of trait means is 0.02 (29 cases, or half a percent), and 0.01 (13 cases, or quarter of a percent). Figure 18 shows examples from our data where pairs of species evolved very similar trait means.

The biological interpretation of the inequalities (3.28) and (3.29) necessary for two-species trait convergence were that trait variances must be sufficiently different, and the fitness landscape at the point of convergent evolution should be sufficiently sharply changing. The second of these conditions is most easily achieved when $\sigma \approx \theta$, and indeed, that was when we observed trait convergence in the two-species scenarios (Section 3.3). However, in our multispecies communities, the trait variances are always considerably smaller than θ (compare Figure 18 with Figure 10). The only way to achieve the required sharply changing fitness landscape is through frequency-dependent effects, such as interactions with flanking species from either side. The resulting landscape will likely not be perfectly symmetric, but the effect of a small asymmetry is simply to shift the trait means slightly away from strict equality (Section 3.4).

Since to get trait convergence the two trait variances need to be sufficiently different, one would think that most simulations where convergence was observed had mixed levels of intraspecific variation (intraspecific standard deviations uniformly sampled from $[0.01, 0.3]$; this distribution has the largest variance of the σs). This is indeed the case: out of the 60 cases where the minimum trait difference was less than 0.03, 41 had mixed levels of variation (68%); out of the 29 with minimum difference less than 0.02, 24 (83%); and out of the 13 with minimum difference below 0.01, 10 (77%).

Since the conditions for trait convergence are somewhat restrictive, we do not expect it to happen very often. Our simulation results show that, while convergence is definitely a rare event, it still happens occasionally. However, measured by its effect on our community metrics (Section 4.3), trait convergence does not appear to be a very strong force in shaping community structure.

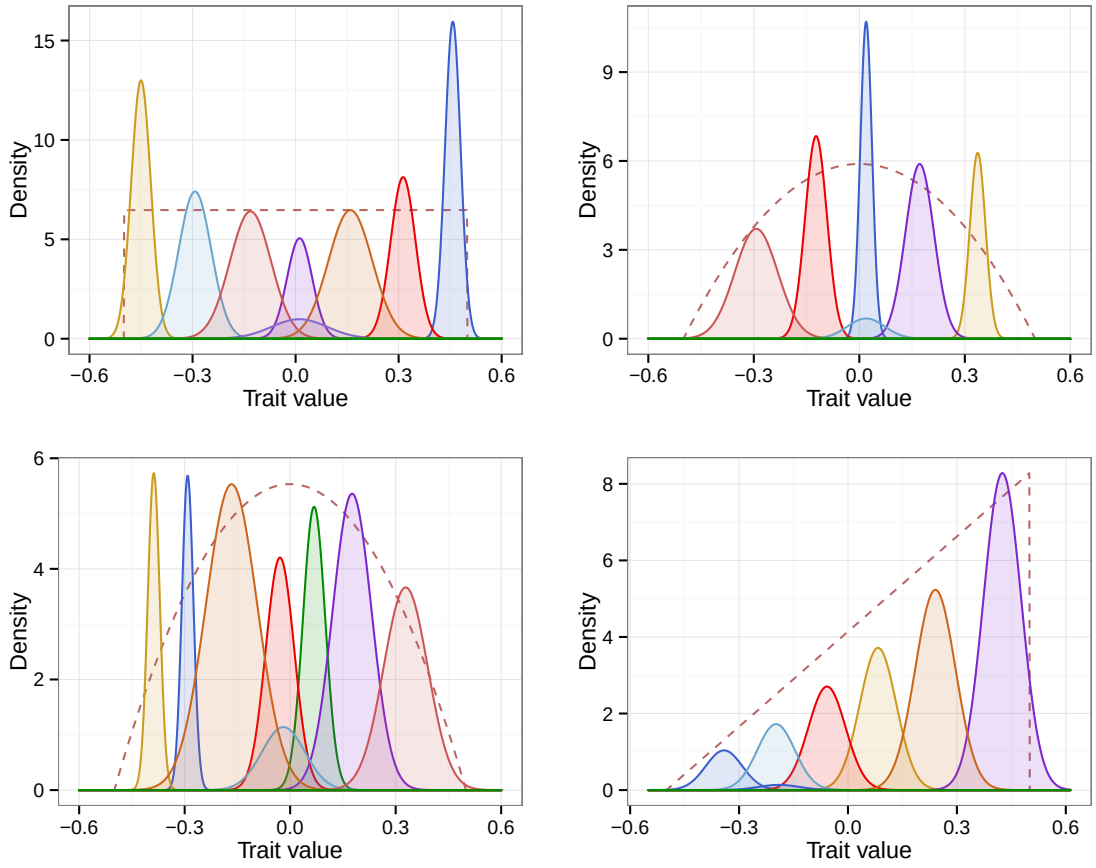

Figure 18: Simulation results with $h^2 > 0$ where the final community has species with mean trait difference less than 0.01 units along the trait axis. The dashed lines (not drawn to scale) depict the shape of the intrinsic growth function.

5 Relaxing the assumptions of the extreme quantitative genetic limit: the Shpak-Kondrashov model

So far all our results were obtained under the assumption that the ecologically relevant trait z in question is determined by the sum of a random, normally distributed environmental noise, and a genetic component with infinitely many loci contributing to the trait, each locus having an infinitesimal additive effect. Under these assumptions, the intraspecific trait distribution is normal and selection can only change its mean, not the higher moments (see Section 1). Here we check the robustness of our results to relaxing the assumption of infinitely many loci.

One way of doing this would be to do a purely individual-based simulation. The disadvantage to this is that such simulations are very expensive computationally. A convenient middle ground is provided by the Shpak-Kondrashov hypergeometric model (Shpak and Kondrashov 1999, Yamauchi and Miki 2009). In this model the trait of interest is coded by n additive loci in a diploid, sexually reproducing population. The probability R^u_{vw} that two parents with genotypes v and w give birth to an offspring with genotype u is modeled via

$$R^u_{vw} = \sum_{s=0}^{v} H(v, \max(v, s+v-2n))\, H(w, \max(w, u+w-s-2n)), \tag{5.1}$$

where

$$H(u,v) = \frac{\binom{u}{v}\binom{u}{v-u}}{\binom{2u}{u}} \tag{5.2}$$

is the hypergeometric distribution. This model is accurate as long as the allelic composition of every phenotype is in linkage equilibrium. When recombination is free, mating is random, and selection only depends on phenotype, no within-phenotype linkage disequilibrium will evolve as long as there was none initially (Shpak and Kondrashov 1999). Since in our Lotka–Volterra ecological models selection is a function of phenotype, the hypergeometric model's assumptions hold as long as there is no initial linkage disequilibrium within phenotypes.

5.1 Community model with no environmental effect on phenotype

At first let us assume that genotype fully determines phenotype, i.e., there is no environmental component to the total phenotypic variance, making heritability equal to 1. Let the population density of species i's genotype u at time t be $N_{iu}(t)$. Assuming a short time slice Δt, let the same densities be $N'_{iu}(t)$ after selection, and then $N_{iu}(t+\Delta t)$ after reproduction. Selection happens via Lotka–Volterra dynamics:

$$N'_{iu}(t) = N_{iu}(t) - \Delta t N_{iu}(t) \sum_v \sum_j a_{uv} N_{jv}(t), \tag{5.3}$$

where a_{uv} is the competitive effect of individuals with genotype v on those with genotype u. Given the trait values z and z' associated with these genotypes, the competition coefficients are given by Eq. (2.18). Since we assume that all species have the same genetic structure, these coefficients are independent of species identity.

For reproduction, if the density-independent growth rate of species i's genotype u is b_{iu}, and the offspring genotype frequencies are given by the hypergeometric model, we can write

$$N_{iu}(t+\Delta t) = N'_{iu}(t) + \Delta t\, b_{iu} c_i^{-1} \sum_v \sum_w R^u_{vw} N'_{iv}(t) N'_{iw}(t) \tag{5.4}$$

for the densities after the time slice Δt. Here c_i^{-1} simply ensures proper normalization:

$$c_i = \sum_u \sum_v \sum_w R^u_{vw} N_{iv}(t) N_{iw}(t). \tag{5.5}$$

Putting Eqs. (5.3) and (5.4) together, we get

$$N_{iu}(t+\Delta t) = \left(N_{iu}(t) + \Delta t\, b_{iu} c_i^{-1} \sum_v \sum_w R^u_{vw} N_{iv}(t) N_{iw}(t) \right) \left(1 - \Delta t \sum_v \sum_j a_{uv} N_{jv}(t) \right). \tag{5.6}$$

Neglecting higher order terms, subtracting $N_{iu}(t)$ from both sides, dividing by Δt, and taking the $\Delta t \to 0$ limit, we arrive at

$$\frac{\mathrm{d}N_{iu}(t)}{\mathrm{d}t} = b_{iu} c_q^{-1} \sum_v \sum_w R^u_{vw} N_{iv}(t) N_{iw}(t) - N_{iu}(t) \sum_v \sum_j a_{uv} N_{jv}(t), \tag{5.7}$$

the differential equation governing genotype u of species i, assuming that genotype perfectly determines phenotype. Note that the number of equations is the number of species times the number of possible genotypes; for instance, with $S = 51$ species and $n = 25$ loci (leading to $2n+1 = 51$ distinct genotypes), the number of differential equations is $51 \times 51 = 2601$. This is computationally much more expensive than simulating the quantitative genetic limit. For this reason, we do not perform the same extensive simulations

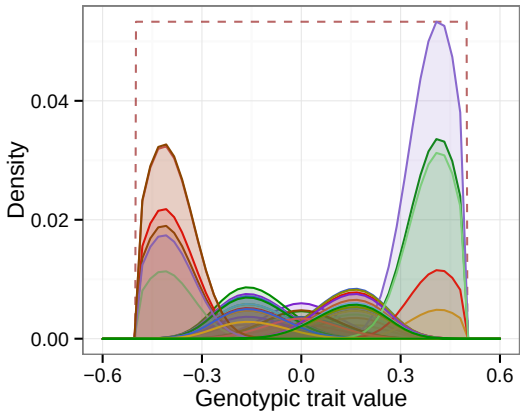

Figure 19: Final state of species' trait distributions (shaded regions) from simulating Eq. (5.7) with $\omega = 0.1$, $S = 51$ diploid species, and random initial conditions. Each species has $n = 25$ additive loci, each with two possible alleles ("0" and "+"), for a total of $2n+1 = 51$ different genotypic values. We assume a species has trait -0.6 if all its loci are equal to "0", and every "+" locus contributes 0.024 units to the trait value; i.e., the maximum possible trait value is $50 \times 0.024 - 0.6 = 0.6$. We assume b_{iu} depends only on the genotypic value u: $b_{iu} = 1$ if u is such that the phenotypic value is between ± 0.5 and zero otherwise (red dashed line; not drawn to scale). Species' trait distributions are approximately normal even close to the edges of the trait axis, where there is strong, externally imposed selection acting. Since the finite number of loci effectively discretizes the trait axis into 51 bins, and all species have the exact same genetic structure, once two species evolve the same phenotypic distribution, they become completely identical with no competitive exclusion between them. This is exactly what we see on the figure: there are five well-defined regions along the axis where species can persist, but each region is occupied by several identical, neutrally coexisting "species".

as before. Instead, we simulate a few scenarios to see whether the results are qualitatively the same as in the quantitative genetic limit.

Figure 19 shows a sample run of this model with 51 diploid species, each with $n = 25$ additive loci. Note that approximately normal trait distributions are maintained even under strong, constant selection. The qualitative result is the same as in the extreme quantitative genetic limit; the only difference is that, since genotype is the only determinant of phenotype, and all species share the same genetic system, species may evolve to have identical phenotypic distributions, thus effectively morphing into the same species. This convergent evolution is enhanced by the effective discretization of the trait space, since for n additive loci only $2n+1$ different trait values are possible. Once two species achieve the same genotype (and therefore phenotype) distribution, they are, for all intents and purposes, the same species, the differences in their phylogenetic histories completely erased.

5.2 Community model with environmental effects on phenotype

To allow for heritabilities different from one, we assume that there is species-specific Gaussian environmental noise on top of the trait values determined by the genotypes. The distribution $p_{iu}(z)$ of the phenotype values of species i's genotype u then reads

$$p_{iu}(z) = \sqrt{\frac{1}{2\pi\sigma_{E,i}^2}} \exp\left(-\frac{(\mu_{iu}-z)^2}{2\sigma_{E,i}^2}\right), \tag{5.8}$$

where μ_{iu} is the mean phenotypic trait of species i's genotype u (i.e., what it would always be in the absence of environmental noise), which does not depend on time. The variance $\sigma_{E,i}^2$ is species-specific. Instead of

$N_{iu}(t)$, we now have $N_{iu}(z,t)$, which is the trait distribution of species i's genotype u:

$$N_{iu}(z,t) = N_{iu}(t)p_{iu}(z) = N_{iu}(t)\sqrt{\frac{1}{2\pi\sigma_{E,i}^2}}\exp\left(-\frac{(\mu_{iu}-z)^2}{2\sigma_{E,i}^2}\right). \tag{5.9}$$

The integral of this distribution along the whole trait axis is

$$\int N_{iu}(z,t)\,\mathrm{d}z = N_{iu}(t)\int p_{iu}(z)\,\mathrm{d}z = N_{iu}(t), \tag{5.10}$$

as it should be.

The competition term of Eq. (5.7) needs to be modified because individuals compete via their traits and not their genotypes. Taking this into account, Eq. (5.7) is modified to read

$$\frac{\mathrm{d}N_{iu}(z,t)}{\mathrm{d}t} = b(z)p_{iu}(z)c_i^{-1}\sum_v\sum_w R_{vw}^u N_{iv}(t)N_{iw}(t) - N_{iu}(z)(t)\int a(z,z')\sum_v\sum_j N_{jv}(z',t)\,\mathrm{d}z'. \tag{5.11}$$

We integrate both sides across z. The left hand side is simply

$$\int \frac{\mathrm{d}N_{iu}(z,t)}{\mathrm{d}t}\,\mathrm{d}z = \frac{\mathrm{d}}{\mathrm{d}t}\int N_{iu}(z,t)\,\mathrm{d}z = \frac{\mathrm{d}N_{iu}(t)}{\mathrm{d}t}, \tag{5.12}$$

while the right hand side is

$$\int b(z)p_{iu}(z)\,\mathrm{d}z\,c_i^{-1}\sum_v\sum_w R_{vw}^u N_{iv}(t)N_{iw}(t) - N_{iu}(t)\sum_v\sum_j N_{jv}(t)\iint p_{iu}(z)a(z,z')p_{jv}(z')\,\mathrm{d}z'\mathrm{d}z. \tag{5.13}$$

Defining

$$b_{iu} = \int b(z)p_{iu}(z)\,\mathrm{d}z \tag{5.14}$$

and

$$a_{iujv} = \iint p_{iu}(z)a(z,z')p_{jv}(z')\,\mathrm{d}z'\mathrm{d}z, \tag{5.15}$$

the final form of the equation reads

$$\frac{\mathrm{d}N_{iu}(t)}{\mathrm{d}t} = b_{iu}c_i^{-1}\sum_v\sum_w R_{vw}^u N_{iv}(t)N_{iw}(t) - N_{iu}(t)\sum_v\sum_j a_{iujv}N_{jv}(t). \tag{5.16}$$

This has the same form as Eq. (5.7), except the two-index a_{uv} is replaced with the four-index a_{iujv}, which depends not only on the genotypes, but also the environmental variances of species i and j. These ingredient functions can be integrated just like in Sections 2.3 and 2.3. Assuming a rectangular $b(z)$ given by Eq. (2.21) and a Gaussian $a(z,z')$ given by Eq. (2.18), we get

$$b_{iu} = \frac{1}{2}\left[\mathrm{erf}\left(\frac{\theta-\mu_{iu}}{\sqrt{2}\sigma_{E,i}}\right) + \mathrm{erf}\left(\frac{\theta+\mu_{iu}}{\sqrt{2}\sigma_{E,i}}\right)\right], \tag{5.17}$$

$$a_{iujv} = \frac{\omega}{\sqrt{2\sigma_{E,i}^2+2\sigma_{E,j}^2+\omega^2}}\exp\left(-\frac{(\mu_{iu}-\mu_{jv})^2}{2\sigma_{E,i}^2+2\sigma_{E,j}^2+\omega^2}\right). \tag{5.18}$$

Note also that Eq. (5.16) collapses into Eq. (5.7) in the limit of all $\sigma_{E,i}^2$ going to zero.

Adding an environmental component to species' phenotypic variances breaks the perfect symmetry of the species in that now even if two species evolve the exact same genotype distribution, their trait distributions will be different (unless their environmental variances are precisely equal). Because of this, species retain their identity even if they undergo convergent evolution, and cannot become identical. In this scenario therefore, we end up with communities that look very much like those obtained under the quantitative genetic limit (Figure 20, left panel). This is despite the fact that, since the amount of within-species genetic variation changes through time, species' heritabilities are also no longer constant, and are no longer equal across species.

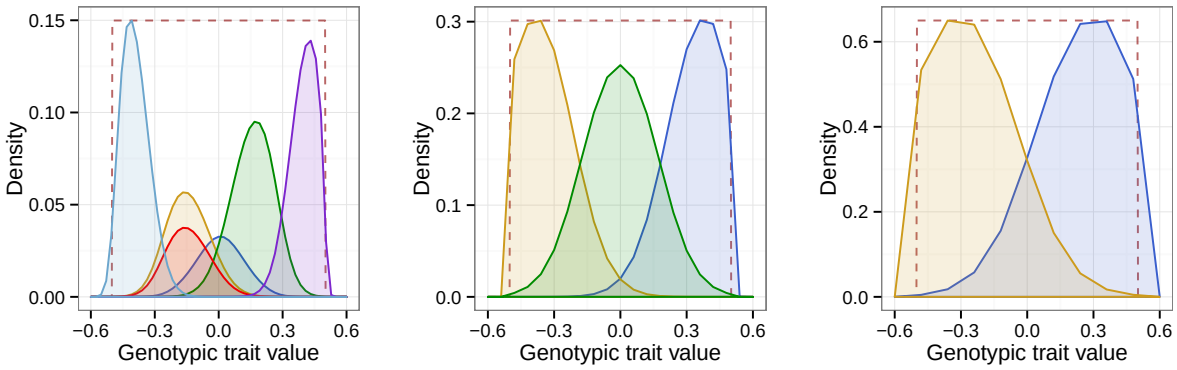

Figure 20: As Figure 19, except all species have an environmental component to their phenotypic variance. Only the genotypic trait values are plotted. The number of loci is $n = 25$ on the left, $n = 10$ in the center, and $n = 5$ on the right panel. The species-specific environmental standard deviations $\sigma_{E,i}$ were sampled uniformly and independently from the interval $[0.01, 0.05]$. Their values for the six surviving species on the left panel are: 0.029 (light blue), 0.034 (yellow), 0.017 (red), 0.046 (blue), 0.027 (green), 0.028 (purple). The $\sigma_{E,i}$ in the center are: 0.010 (yellow), 0.012 (green), and 0.013 (blue). The $\sigma_{E,i}$ on the right: 0.010 (yellow), and 0.014 (blue). Species now cannot evolve the exact same phenotype distribution, because even if their genetic makeup is identical, environmental noise will affect their traits differently (except in the nongeneric case of precisely equal environmental variances). Due to this fact, convergent evolution as in Figure 19 is only possible if there is a generalist-specialist distinction between the species (Section 3.2). Therefore, only a handful of species survive out of the initial 51, in line with model results in the quantitative genetic limit.

The quantitative genetic assumption of infinitely many loci can be violated even more and one still gets similar results. Reducing the number of loci to $n = 10$, or even to a mere $n = 5$ (Figure 20, center and right panels), the trait distributions are still close to being normal. Since the possible genotypic trait values still run between ± 0.6 but the number of possible genotypes is only $2n + 1$, a single allele now contributes 0.06 ($n = 10$) or 0.12 ($n = 5$) units to the trait value, instead of the previous 0.04 with $n = 25$. This implies that the phenotypic variance will be much larger, even without the added environmental component. As discussed in Section 4.1, this also means reduced species richness, which is exactly what we see on Figure 20.

In conclusion, relaxing the assumption of infinitely many loci with infinitesimal additive effects does not seem to fundamentally alter the results obtained under the quantitative genetic limit, even when the number of loci is small and their phenotypic effects are large.

6 Competition along two independent trait dimensions

Up to this point we have assumed that a single ecologically relevant trait governs the interactions between individuals of the community. Here we perform a preliminary exploration of the effects of having multiple independent trait axes.

Let us assume there are two independent quantitative traits z_1 and z_2. For simplicity, we also assume that species' trait distributions have the same variance σ_i^2 along both directions. The normalized bivariate trait distribution then reads

$$p_i(\vec{z}) = \frac{1}{2\pi\sigma_i^2}\exp\left(-\frac{\|\vec{z}-\vec{\mu}_i\|^2}{2\sigma_i^2}\right) = \frac{1}{2\pi\sigma_i^2}\exp\left(-\frac{(z_1-\mu_{i1})^2+(z_2-\mu_{i2})^2}{2\sigma_i^2}\right), \tag{6.1}$$

where $\vec{z} = (z_1, z_2)$ and $\vec{\mu}_i = (\mu_{i1}, \mu_{i2})$ are vectors in trait space, and $\|\cdot\|$ is the Euclidean norm. Competition is assumed to depend only on distance, and so is given by

$$a(\vec{z},\vec{z}') = \exp\left(-\frac{\|\vec{z}-\vec{z}'\|^2}{\omega^2}\right) = \exp\left(-\frac{(z_1-z_1')^2+(z_2-z_2')^2}{\omega^2}\right). \tag{6.2}$$

We use the rectangular growth function in two dimensions:

$$b(\vec{z}) = \begin{cases} 1 & \text{if } \max(|z_1|,|z_2|) \le \theta, \\ 0 & \text{otherwise.} \end{cases} \tag{6.3}$$

The fitness of an individual with phenotype $\vec{z}$ is given by

$$r(\vec{N},\vec{p},\vec{z}) = b(\vec{z}) - \sum_{j=1}^{S} N_j \int a(\vec{z},\vec{z}')p_j(\vec{z}')\,\mathrm{d}\vec{z}', \tag{6.4}$$

the multidimensional generalization of Eq. 2.1 (here and onwards, we suppress the time-dependence of quantities for notational convenience).

The effective competition coefficients are still given by Eq. (2.4), but integrated over the whole trait space. Evaluating the integral yields

$$\alpha_{ij} = \iint p_i(\vec{z})a(\vec{z},\vec{z}')p_j(\vec{z}')\,\mathrm{d}\vec{z}\,\mathrm{d}\vec{z}' = \frac{\omega^2}{\omega^2+2\sigma_i^2+2\sigma_j^2}\exp\left(-\frac{(\mu_{i1}-\mu_{j1})^2+(\mu_{i2}-\mu_{j2})^2}{\omega^2+2\sigma_i^2+2\sigma_j^2}\right). \tag{6.5}$$

The effective growth rates are similarly given by Eq. (2.3) but integrated over $\vec{z}$. With the rectangular growth function in Eq. (6.3), the integral gives

$$b_i = \int b(\vec{z})p_i(\vec{z})\,\mathrm{d}\vec{z} = \frac{1}{4}\left[\mathrm{erf}\left(\frac{\theta-\mu_{i1}}{\sqrt{2}\sigma_i}\right)+\mathrm{erf}\left(\frac{\theta+\mu_{i1}}{\sqrt{2}\sigma_i}\right)\right]\left[\mathrm{erf}\left(\frac{\theta-\mu_{i2}}{\sqrt{2}\sigma_i}\right)+\mathrm{erf}\left(\frac{\theta+\mu_{i2}}{\sqrt{2}\sigma_i}\right)\right]. \tag{6.6}$$

The time evolution of the abundances follows the multidimensional generatization of Eq. (1.18):

$$\frac{\mathrm{d}N_i}{\mathrm{d}t} = N_i\int r_i(\vec{N},\vec{p},\vec{z})p_i(\vec{z})\,\mathrm{d}\vec{z} = N_i\left(b_i - \sum_{j=1}^{S}\alpha_{ij}N_j\right). \tag{6.7}$$

We can obtain the multidimensional versions of $\bar{b}_i$ (Eq. 2.7) and β_{ij} (Eq. 2.8) analogously:

$$\begin{aligned}\vec{\bar{b}}_i &= \int(\vec{z}-\vec{\mu}_i)p_i(\vec{z})b(\vec{z})\,\mathrm{d}\vec{z} \\ &= \begin{pmatrix} \dfrac{\sigma_i}{2\sqrt{2\pi}}\exp\left(-\dfrac{(\theta+\mu_{i1})^2}{2\sigma_i^2}\right)\left[1-\exp\left(\dfrac{2\theta\mu_{i1}}{\sigma_i^2}\right)\right]\left(\mathrm{erf}\left(\dfrac{\theta-\mu_{i2}}{\sqrt{2}\sigma_i}\right)+\mathrm{erf}\left(\dfrac{\theta+\mu_{i2}}{\sqrt{2}\sigma_i}\right)\right) \\ \dfrac{\sigma_i}{2\sqrt{2\pi}}\exp\left(-\dfrac{(\theta+\mu_{i2})^2}{2\sigma_i^2}\right)\left[1-\exp\left(\dfrac{2\theta\mu_{i2}}{\sigma_i^2}\right)\right]\left(\mathrm{erf}\left(\dfrac{\theta-\mu_{i1}}{\sqrt{2}\sigma_i}\right)+\mathrm{erf}\left(\dfrac{\theta+\mu_{i1}}{\sqrt{2}\sigma_i}\right)\right) \end{pmatrix},\end{aligned} \tag{6.8}$$

and

$$\begin{aligned}\vec{\beta}_{ij} &= \iint (\vec{z}-\vec{\mu}_i)p_i(\vec{z})a(\vec{z},\vec{z}')p_j(\vec{z}')\,\mathrm{d}\vec{z}\,\mathrm{d}\vec{z}' \\ &= -\frac{2\omega^2\sigma_i^2(\vec{\mu}_i-\vec{\mu}_j)}{\left(\omega^2+2\sigma_i^2+2\sigma_j^2\right)^2}\exp\left(-\frac{(\mu_{i1}-\mu_{j1})^2+(\mu_{i2}-\mu_{j2})^2}{\omega^2+2\sigma_i^2+2\sigma_j^2}\right).\end{aligned} \tag{6.9}$$

The time evolution of the trait means $\vec{\mu}_i$ is given by the generalization of Eq. (1.23):

$$\frac{\mathrm{d}\vec{\mu}_i}{\mathrm{d}t} = G\int(\vec{z}-\vec{\mu}_i)r_i(\vec{N},\vec{p},\vec{z})p_i(\vec{z})\,\mathrm{d}\vec{z} = G\left(\vec{\bar{b}}_i - \sum_{j=1}^{S}\vec{\beta}_{ij}N_j\right), \tag{6.10}$$

where G is the genetic variance-covariance matrix (Lande 1982). Since there are two traits, here G is a 2×2 matrix.

This two-dimensional model can be simulated just like the original one. We use the simplest assumption of ecologically and genetically independent traits with equal heritability h^2 between species and along both trait axes. This means that the variance-covariance matrix is simply $G = h^2 I$ for all species, where I is the 2×2 identity matrix. The initial number of species is $S = 51$, their initial population densities are all equal to one, and both coordinates of the initial trait positions are uniformly sampled from $[-\theta, \theta]$. We set $\omega = 0.2$, $\theta = 1/2$, and $h^2 = 0.1$ when species can evolve or $h^2 = 0$ when they cannot. Intraspecific standard deviations are uniformly sampled from $[0.05, 0.2]$ (in the presence of intraspecific variation), or are all set to $\sigma_i = 0.005$ (much smaller than θ and the competition width, effectively meaning the lack of any intraspecific variation).

Results of sample simulations are seen on Figures 21 (no intraspecific variation), 22 (nonheritable variation), and 23 (heritable variation). Results are very much in line with what we have seen for a single trait dimension. Species richness declines with increasing intraspecific variability, and further so with nonzero heritability. Mean traits in the zero heritability cases seem to be more evenly spaced than random, though this needs to be tested rigorously. However, there is a very clear even pattern when heritability is positive. Importantly, these patterns are only visible when the entire two-dimensional trait space is considered. Projecting the trait distributions onto just one of the axes, one sees lots of between-species overlap, and no pattern of even spacing at all. In fact, the opposite may be argued: species appear to be more clustered than random, which makes sense in light of the full two-dimensional trait distributions. Whether this signature of extra clustering is detectable in empirical data, or whether it would still be present if the number of trait axes was much larger than two, are open questions.

In summary, our results appear to be fundamentally unchanged by including multiple trait dimensions. As long as one looks for patterns in the whole trait space and not just a projection onto a single axis, the same expectations of reduced species richness and even spacing are found as before.

7 Code

The code we used to generate our results, along with documentation, can be accessed and downloaded either from the Ecology Letters website, or from https://github.com/dysordys/intravar.

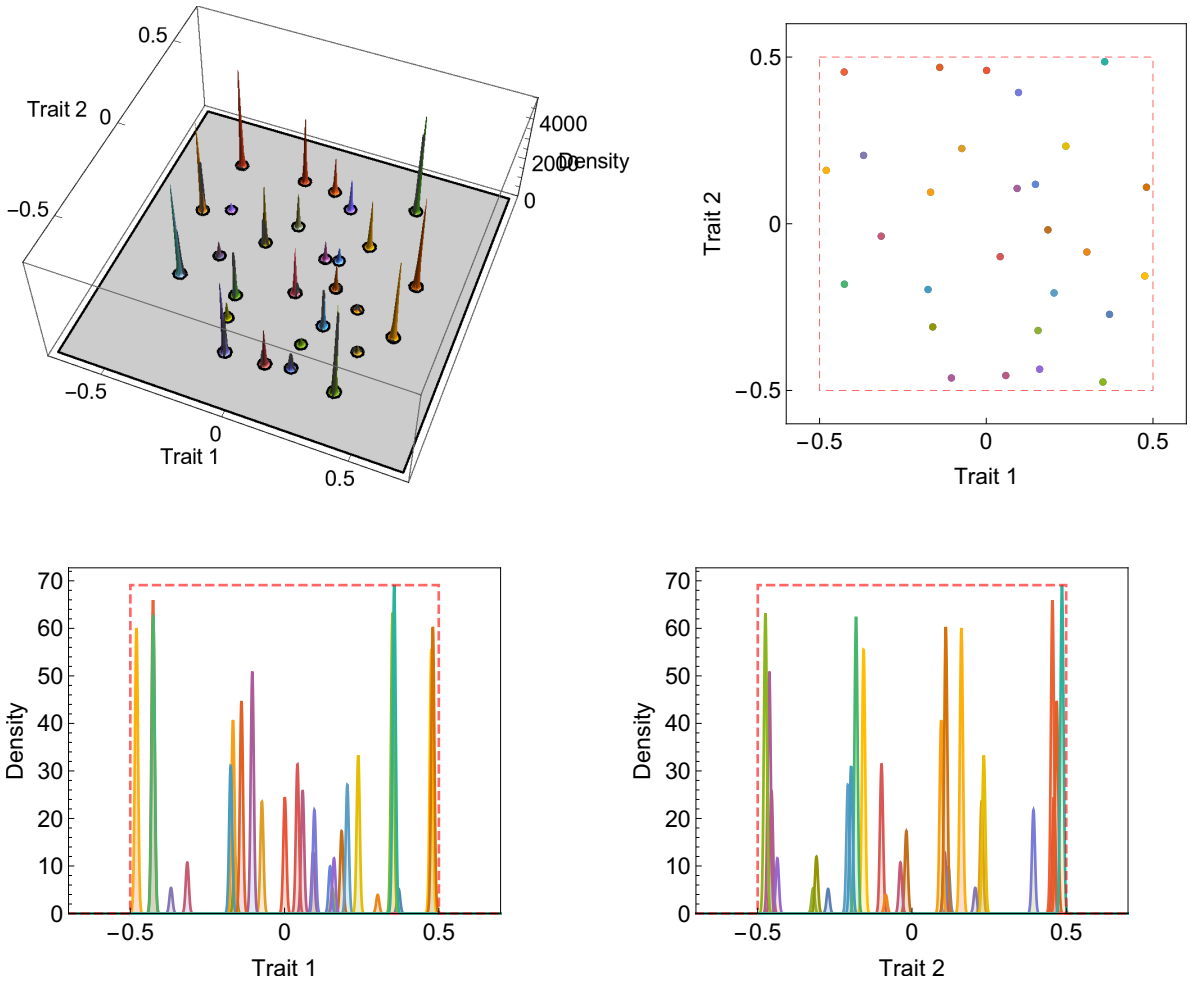

Figure 21: Final state of community with two trait axes instead of just one. This is the case with no intraspecific variation; $h^2 = 0$. Out of the initial 51 species, 28 survive. Their traits are more or less evenly distributed in phenotypic space (top, with the full trait distributions on the left and mean trait positions from a bird's eye view, without abundance information, on the right). When this gets projected onto just a single trait axis at a time (bottom, with projection onto the first axis on the left and onto the second on the right), the patterns look much more random. Red dashed lines (not to scale) show the growth function $b(z)$.

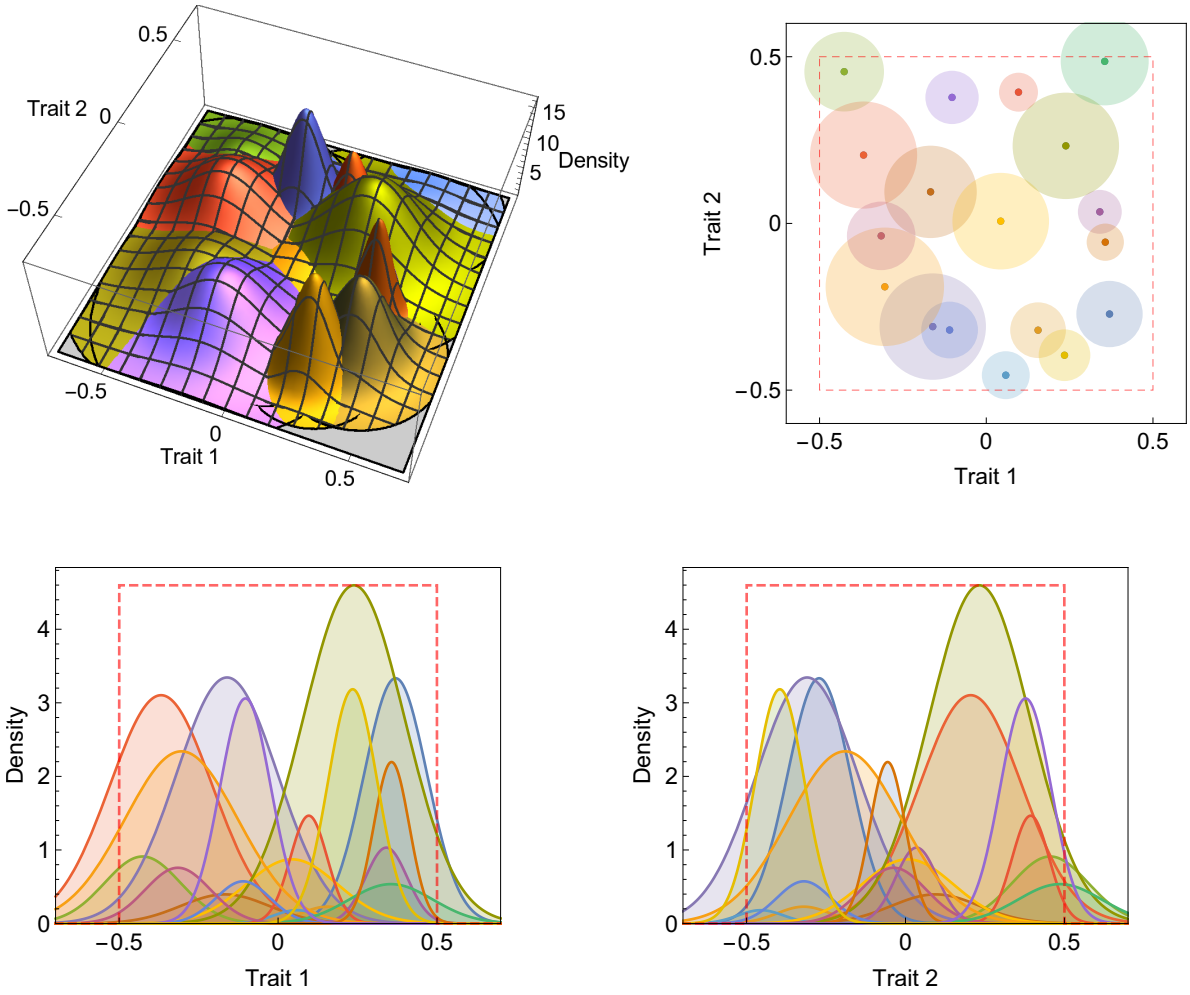

Figure 22: As Figure 21, but with species' intraspecific standard deviations uniformly sampled from $[0.05, 0.2]$; $h^2 = 0$. Transparent disks on the top right mark one standard deviation of species' trait distributions. Out of the initial 51 species, 18 survive. Again, a pattern that looks more even than random (top) is obscured by projecting onto a single trait axis (bottom).

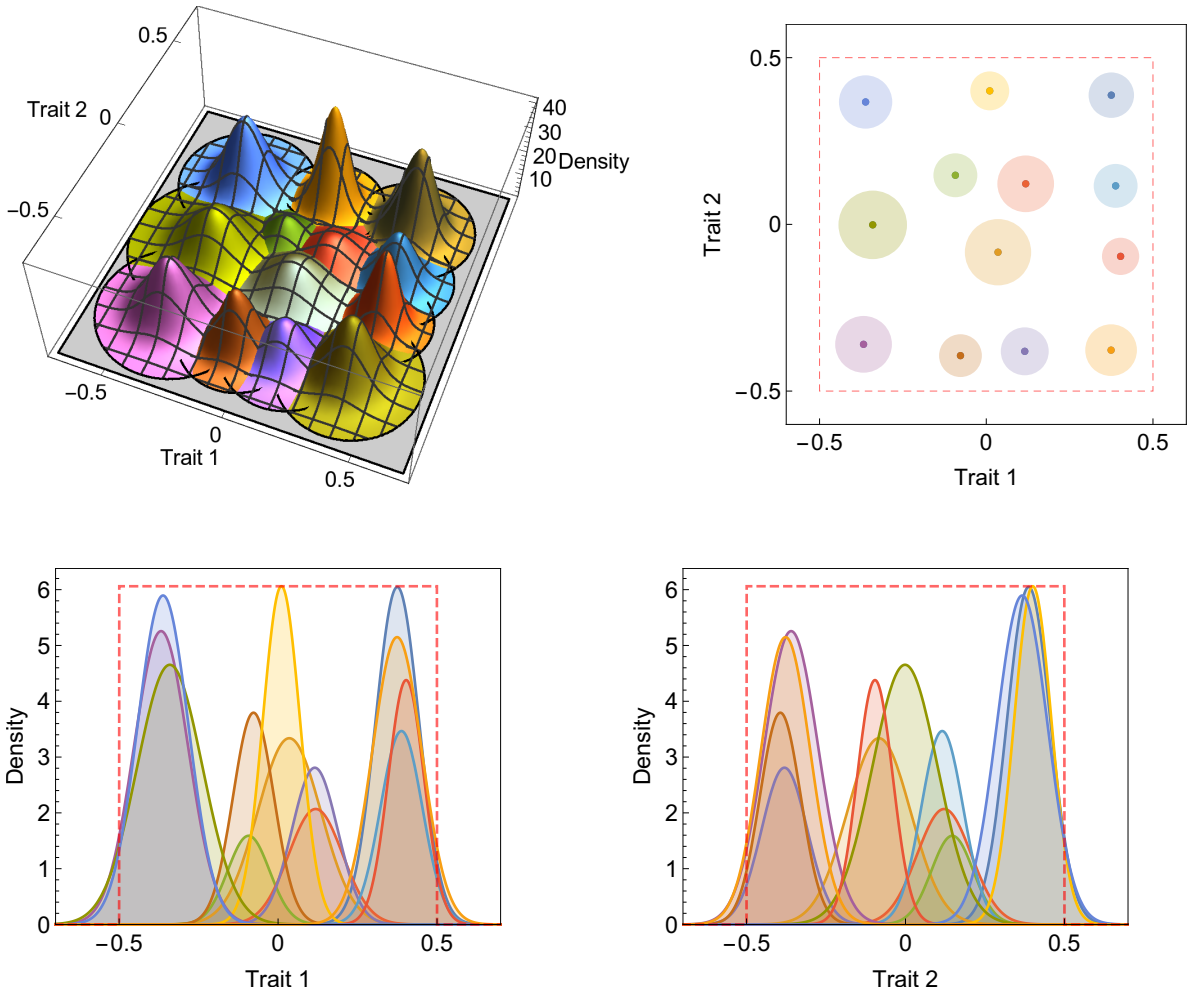

Figure 23: As Figure 22, but with $h^2 = 0.1$. Out of the initial 51 species, 13 survive. This time the regular pattern is obvious in the whole trait space (top). However, this is still obscured when projected onto any single axis (bottom), where species appear to have substantial trait overlap.

References

Aufderheide, H., Rudolf, L., Gross, T., Lafferty, K. D., 2013. How to predict community responses to perturbations in the face of imperfect knowledge and network complexity. Proceedings of the Royal Society of London Series B 280, 20132355.

Barabás, G., Meszéna, G., 2009. When the exception becomes the rule: the disappearance of limiting similarity in the Lotka–Volterra model. Journal of Theoretical Biology 258, 89–94.

Barabás, G., Meszéna, G., Ostling, A., 2014a. Fixed point sensitivity analysis of interacting structured populations. Theoretical Population Biology 92, 97–106.

Barabás, G., Pásztor, L., Meszéna, G., Ostling, A., 2014b. Sensitivity analysis of coexistence in ecological communities: theory and application. Ecology Letters 17, 1479–1494.

Barabás, G., Pigolotti, S., Gyllenberg, M., Dieckmann, U., Meszéna, G., 2012. Continuous coexistence or discrete species? A new review of an old question. Evolutionary Ecology Research 14, 523–554.

Bender, E. A., Case, T. J., Gilpin, M. E., 1984. Perturbation experiments in community ecology: Theory and practice. Ecology 65, 1–13.

Bolnick, D. I., Amarasekare, P., Araújo, M. S., Bürger, R., Levine, J. M., Novak, M., Rudolf, V. H. W., Schreiber, S. J., Urban, M. C., Vasseur, D. A., 2011. Why intraspecific trait variation matters in community ecology. Trends in Ecology and Evolution 26, 183–192.

Bulmer, M. G., 1980. The mathematical theory of quantitative genetics. Clarendon Press, Oxford, UK.

Bürger, R., 2011. Some mathematical models in evolutionary genetics. In: FACC Chalub, Rodrigues, J. F. (Eds.), The Mathematics of Darwins Legacy. Birkhäuser, Basel, pp. 67–89.

Dambacher, J. M., Li, H. W., Rossignol, P. A., 2002. Relevance of community structure in assessing indeterminacy of ecological predictions. Ecology 83, 1372–1385.

Edelstein-Keshet, L., 1988. Mathematical models in biology. Random House, New York, USA.

Falconer, D. S., 1981. Introduction to Quantitative Genetics. Longman, London.

Lande, R., 1976. Natural selection and random genetic drift in phenotypic evolution. Evolution 30, 314–334.

Lande, R., 1982. A quantitative genetic theory of life history evolution. Ecology 63, 607–615.

Levins, R., 1968. Evolution in changing environments. Princeton University Press, Princeton.

Levins, R., 1974. Qualitative analysis of partially specified systems. Ann. NY Acad. Sci. 231, 123–138.

MacArthur, R. H., 1970. Species packing and competitive equilibria for many species. Theoretical Population Biology 1, 1–11.

MacArthur, R. H., Levins, R., 1967. Limiting similarity, convergence, and divergence of coexisting species. American Naturalist 101 (921), 377–385.

Mallet, J., 2012. The struggle for existence: how the notion of carrying capacity, K, obscures the links between demography, Darwinian evolution, and speciation. Evolutionary Ecology Research 14, 627–665.

May, R. M., 1973. Stability and Complexity in Model Ecosystems. Princeton University Press, Princeton.

Meszéna, G., Gyllenberg, M., Pásztor, L., Metz, J. A. J., 2006. Competitive exclusion and limiting similarity: a unified theory. Theoretical Population Biology 69, 68–87.

Nagylaki, T., 1992. Introduction to theoretical population genetics. Springer-Verlag, Berlin.

Novak, M., Wootton, J. T., Doak, D. F., Emmerson, M., Estes, J. A., Tinker, M. T., 2011. Predicting community responses to perturbations in the face of imperfect knowledge and network complexity. Ecology 92, 836–846.

Scheffer, M., van Nes, E., 2006. Self-organized similarity, the evolutionary emergence of groups of similar species. Proceedings of the National Academy of Sciences of the USA 103, 6230–6235.

Schreiber, S. J., Bürger, R., Bolnick, D. I., 2011. The community effects of phenotypic and genetic variation within a predator population. Ecology 92, 1582–1593.

Shpak, M., Kondrashov, A. S., 1999. Applicability of the hypergeometric phenotypic model to haploid and diploid populations. Evolution 53, 600–604.

Slatkin, M., 1979. Frequency- and density-dependent selection on a quantitative character. Genetics 93, 755–771.

Slatkin, M., 1980. Ecological character displacement. Ecology 6, 163–177.

Szabó, P., Meszéna, G., 2006. Limiting similarity revisited. Oikos 112, 612–619.

Taper, M. L., Case, T. J., 1985. Quantitative genetic models for the coevolution of character displacement. Ecology 66, 355–371.

Taper, M. L., Case, T. J., 1992. Models of character displacement and the theoretical robustness of taxon cycles. Evolution 46, 317–333.

Vandermeer, J. H., 1975. Interspecific competition: A new approach to the classical theory. Science 188, 253–255.

Vasseur, D. A., Amarasekare, P., Rudolf, V. H. W., Levine, J. M., 2011. Eco-evolutionary dynamics enable coexistence via neighbor-dependent selection. American Naturalist 178, E96–E109.

Yamauchi, A., Miki, T., 2009. Intraspecific niche flexibility facilitates species coexistence in a competitive community with a fluctuating environment. Oikos 118, 55–66.

Yeakel, J. D., Stiefs, D., Novak, M., Gross, T., 2011. Generalized modeling of ecological population dynamics. Theoretical Ecology 4, 179–194.

Yodzis, P., 1988. The indeterminacy of ecological interactions as perceived through perturbation experiments. Ecology 69, 508–515.

Yodzis, P., 2000. Diffuse effects in food webs. Ecology 81, 261–266.